

# Thermal, Energy, and Indoor Environmental Quality Performance of the PA Hemp House

Submitted to DON Services, Inc.

By

*Ali Memari, Corey Griffin, Hojae Yi, Sarah Klinetob Lowe, Nadia Mirzai, and Mahsa Hashemi*

September 2022



**Pennsylvania Housing Research Center (PHRC)  
Penn State, University Park, Pennsylvania**

---

© 2022 by the Pennsylvania Housing Research Center (PHRC)

All rights reserved. For more information, contact the Pennsylvania Housing Research Center, 206B Sackett Building, University Park, PA 16802.

Published October 2022, First Edition

DISCLAIMER: The Pennsylvania Housing Research Center (PHRC) collaboratively engages with the residential construction industry to catalyze advancements in homebuilding through education, training, innovation, research, and dissemination. The PHRC is housed within the Department of Civil & Environmental Engineering at Penn State. The PHRC conducts operations with the support of numerous agencies, associations, companies, and individuals. Neither the PHRC, nor any of its supporters, makes any warranty, expressed or implied, as to the accuracy or validity of the information contained in this document. Similarly, neither the PHRC, nor its sponsors, assumes any liability for the use of the information and procedures provided in this document. Opinions, when expressed, are those of the authors and do not necessarily reflect the views of either the PHRC or anyone of its sponsors. It would be appreciated, however, if any errors of fact or interpretation or otherwise, could be promptly brought to the attention of PHRC.

If additional information is required, contact:

Ali Memari, Director PHRC  
222 Sackett Building  
University Park, PA 16802

---

## **Table of Contents**

<b>Abstract</b>	<b>1</b>
<b>1. Introduction</b>	<b>2</b>
<b>2. Objectives, Tasks, and Scope</b>	<b>5</b>
<b>3. Background on Hempcrete</b>	<b>6</b>
<b>3.1 Hemp and Hemp Hurd</b>	<b>8</b>
<b>3.2 Lime</b>	<b>8</b>
<b>3.3 Making Hempcrete</b>	<b>8</b>
<b>3.4 Hempcrete Properties</b>	<b>10</b>
<b>3.5 Study Plan and Method</b>	<b>10</b>
<b>4. Thermal Resistance of Walls – Heat Flow Meter Method</b>	<b>11</b>
<b>4.1 Instruments for Thermal Resistance Measurement Study</b>	<b>11</b>
<b>4.2 Heat Flow Meter Methodology</b>	<b>13</b>
<b>4.3 Test Setup for the Heat Flow Meter Method</b>	<b>14</b>
<b>4.4 HFM Test Data and Results</b>	<b>21</b>
<b>5. Energy Performance Evaluation</b>	<b>23</b>
<b>5.1 Overview</b>	<b>23</b>
<b>5.2 Overall Energy Modeling Approach</b>	<b>23</b>
<b>5.3 Wall Modeling Approach</b>	<b>26</b>
<b>5.4 Energy Modeling and Analysis Results</b>	<b>27</b>
<b>5.5 Energy Cost Results</b>	<b>30</b>
<b>6. Indoor Environmental Quality (IEQ) Study</b>	<b>32</b>
<b>7. Summary and Conclusions</b>	<b>37</b>
<b>References</b>	<b>39</b>
<b>Appendix A. Blower Door (Air Leakage) Test</b>	<b>42</b>
<b>Appendix B. Drawings</b>	<b>43</b>
<b>Appendix C. Photos of Retrofitted House Prior to and during Finishing Interior / Exterior Surfaces</b>	<b>52</b>

---

## **Abstract**

Given that over 95% of buildings are residential dwellings, for any meaningful global impact on CO<sub>2</sub> reduction, locally sourced materials, and easy to construct methods are needed for energy-efficient and low-carbon residential buildings. One such promising material is industrial hemp, which allows the production of hempcrete, made up of hemp hurd and fibers mixed with lime and water for use as insulation and light blocks for home building. Given the increasing interest and potentials in growing hemp for various applications, including home building, DON Enterprise, Inc. initiated an effort to retrofit an existing house in New Castle, PA to demonstrate the feasibility of using hemp in the application for home construction. This report focuses on experimentally determining the thermal resistance of the walls of the retrofitted house, measuring the indoor air quality, and developing energy modeling and analysis to evaluate the potential for energy saving when hempcrete is used as the main insulation material in the walls. The report provides some background and understanding related to hemp and hempcrete, as well as various attributes based on the literature review.

---

## 1. Introduction

Because most of the building construction worldwide uses a significant amount of masonry, concrete, and steel, overall, buildings are responsible for a significant amount of energy use and CO<sub>2</sub> generation. More specifically, the production of building materials is responsible for 10% of annual global CO<sub>2</sub> generation, while the operation of buildings (heating, cooling, electricity, etc.) accounts for 27% of CO<sub>2</sub> generation (Architecture 2030, 2022). Such material production has contributed to about 1% annual increase in CO<sub>2</sub> emission since 2010 due to increasing demand for buildings (GABC 2019). Therefore, there is strong demand and push to develop new low-carbon or carbon-capturing construction materials and methods.

Few alternatives are available for traditional load-bearing structural systems such as steel, concrete, masonry, and timber. Furthermore, given that residential buildings constitute almost 95% of buildings, more specifically, 90% single-family and 4.5% multi-family (Potter, 2020), for any meaningful global impact on CO<sub>2</sub> reduction, locally sourced materials and easy-to-construct methods are preferred for home building.

A mixture of hemp fiber, hemp hurd, lime, and water, hempcrete has been shown to have potential in residential construction applications to improve the thermal insulation properties of walls, reduce the consumption of carbon-intensive concrete, and reduce the weight of cement-based structures. For wood-frame home building, hempcrete can be cast (Figure 1), sprayed (Figure 2), or used as prefabricated blocks (Figure 3). Considering that the cultivation of industrial hemp is newly reinstated, hempcrete and related construction materials should be developed as a market-ready product that considers the supply chains, processes, and manufacturing facilities that are to be established in the United States.



Figure 1. Example cast in place hempcrete wall confining studs (Left, Courtesy of American Lime Technology <http://www.americanlimetechnology.com/tradical-hemcrete/>, and Right, Flahiff 2009: <https://inhabitat.com/hemcrete-carbon-negative-hemp-walls-7x-stronger-than-concrete/> ).

---

Figure 2. Example spraying hempcrete between studs (Right, <http://rjinsulation.com/nu-wool-premium-cellulose-insulation/>).



Figure 3. Typical example precast Hempcrete Block Building Construction (Below Left, Courtesy of Wikipedia: <https://en.wikipedia.org/wiki/Hempcrete>; Below Right, <https://www.iso hemp.com/en/hemp-blocks-buildings-hempro-system>).



Pennsylvania is one of the leading states that can grow industrial hemp for the purpose of home building. The study presented here targeted mainly the evaluation of thermal properties and energy performance of a home retrofitted using hempcrete, as well as instrumentally determining indoor air quality. Such efforts leading to R&D documents can eventually help the development of standards, which can be used for inclusion in the building code in the future.

This report reflects the effort by the Penn State research team to study a retrofitted house in New Castle, PA. DON Enterprises, Inc. purchased the subject house, and with the help of another project team, Parsons School of Design, developed the design to retrofit the house, where Figures 4 and 5 show, respectively, the house before and after the retrofit. The hempcrete material used for the retrofit project is shown in Figure 6, illustrating the hemp fiber and hurd as well as a cast block of hempcrete.



Figure 4. House (on the right) located at 506 Spruce Street New Castle, PA before retrofit, ([https://www.zillow.com/homedetails/506-Spruce-St-New-Castle-PA-16101/86510118\\_zpid/](https://www.zillow.com/homedetails/506-Spruce-St-New-Castle-PA-16101/86510118_zpid/)).



Figure 5. House after retrofit.



Figure 6. Example material used for retrofit: Hemp fiber and hard (left); Hempcrete block (right).

---

## **2. Objectives, Tasks, and Scope**

The main objectives of this study include the determination of hempcrete's thermal insulative properties and performance and the resulting impact on utility costs in a residential hempcrete renovation. Accordingly, the project used the experimental Heat Flow Meter method (Lu and Memari 2019, 2022) to determine the in-situ thermal resistance of the retrofitted walls of the subject house. More specifically, the thermal properties of hempcrete as part of the wall on the New Castle PA Hemp House were determined using instruments on the walls of the house, collecting data, and then performing the heat flow meter method to obtain the R-value. To study the effect of the retrofitted house on energy consumption, using data and parameters collected or from the literature, energy modeling of the house was developed using the software BEopt to estimate energy consumption. To illustrate the effect of using hempcrete as the main insulation type in the wall, a comparison was made with the case of the house prior to retrofit, where the walls did not have insulation, and a comparison with the energy consumption assuming the house was retrofitted following the conventional batt insulation solution.

Another aspect of the study was to evaluate the indoor air quality after the construction was completed. Accordingly, instruments consisting of thermometers, humidity sensors, and CO<sub>2</sub> sensors were mounted inside the house to read the parameters of interest and provide readings over a period of several months. The study used the original and as-built drawings of the house for modeling purposes. Reasonable assumptions were made for material properties based on standard modeling practice to estimate the condition of the original house and parameter values prior to retrofit construction.



---

### 3. Background on Hempcrete

Hemp is an industrial non-load bearing variant of cannabis that is grown mainly for its fiber, hurd, and seeds (Figure 7). Because of the long-time ban on growing and doing research related to industrial hemp, it has not been considered as a viable renewable resource for U.S. building products. Recently, such bans are being lifted globally because of the increase in the needs and interests in renewable resources. In the United States, Senate Bill S.2667 by the 115<sup>th</sup> Congress makes hemp producers eligible for the Federal Crop Insurance Program and some USDA research grants (<https://www.congress.gov/bill/115th-congress/senate-bill/2667>). Subsequently, there are substantial needs for research on its processing and utilization to support increased acreage planted. However, according to Popescu (2018), out of 30 countries that now grow industrial hemp, currently, only about 10,000 acres in the US grow this crop, half of the acreage in Canada. However, with the passage of the 2018 Farm Bill, it is expected that the US acreage grows significantly. At the same time, there exists a great need to figure out the usage of industrial hemp to expand markets.



Figure 7. Pictures of hemp plant (left), hemp fiber (center), and vertical section of hemp stock. (Photos courtesy of Forest Concepts LLC.)

From an agricultural crop perspective, the yield of hemp is reported to be quite high (2.5 to 8.7 tons of dry straw per acre), which makes it hard to be matched by any other crop to provide this volume of biomass (Green Home Gnome 2017). Also, the growth rate is fast (about four months), and without the need for much fertilizer for growth and without the need for pesticides, it makes the crop highly profitable for farmers (Popescu 2018).

As far as carbon sequestering is concerned, according to GreenSpec (2019) Tradical (2019), hempcrete sequesters 110 kg of CO<sub>2</sub> per 1 m<sup>3</sup> of hempcrete, considering the carbon emission due to producing the lime binder. Based on another report (Green Home Gnome 2017), on average, a 2000 sq.ft. home would sequester about 5 tons of CO<sub>2</sub> if built using hempcrete. This can be compared with the emission of 1 ton of CO<sub>2</sub> in the production of batt insulation for the same home.

---

While there are some example hempcrete mixture proportions suggested by some builders and industry, some basic material mixture design is needed to develop a thorough understanding of various designs and choose the design that works best for the envisioned system. In general, hempcrete can be made by mixing hemp hurds, lime, sand, plaster, cement, additives, and water (Priesnitz 2006). The proportion of each ingredient should be varied until optimum properties for precast block form and cast-in-place option can be determined. Currently, a standard mixture design has not been developed. Different manufacturers of hempcrete mixture have their own mixture designs. For example, the mixture design by Chanvra Core hurd, which is marketed as KanaBat and distributed in the US by Americhanvre Cast Hemp (Figure 8), is made by mixing the hurds as aggregate with a lime binder, in this case, LCG mortar, Figure 9.



Figure 8. Hemp Hurd (Hemp: <https://chanvra.org/pages/hemp-construction-materials-hempcrete>; A bulk sample of Kanabat Building Grade Hemp Hurd that can be used as alternative aggregate of hempcrete.



Figure 9. Lime used for making hempcrete Lime: <https://www.lcgfrance.com/mortiers-et-enduits-isolants/>; <https://chanvra.org/pages/hemp-construction-materials-hempcrete>).

---

### **3.1 Hemp and Hemp Hurd**

Fibers that make up the exterior surface of hemp stalk have the tensile capacity that is thought to be comparable to steel, and thus are the premium part of the stalk. The woody core hurd can be chopped as shiv and used as a construction aggregate material to create a wall system with high thermal insulation and thermal mass properties.

As hemp grows (as tall as 4.5 m and 25 mm dia.), it absorbs a significant amount of CO<sub>2</sub>, (e.g., 716 lb. (325 kg) of CO<sub>2</sub> in one tonne (1000 kg) of dried hemp) (Green Home Gnome 2017). The greenhouse gas storage properties of hempcrete are impressive, where 1 m<sup>3</sup> of hempcrete can store 165-180 kg CO<sub>2</sub>. Construction of a 300 mm thick hempcrete wall can be a net negative 40 kg CO<sub>2</sub> per square meter of the wall accounting for the emission during hydrated lime production and re-absorption by lime over time.

From an environmental and sustainability perspectives, hemp hurd can essentially be considered a by-product of hemp fiber producers, as they strip the valuable fibers from the hemp stalk, leaving the hurd with no value-added use. Since the use of hemp hurd in hempcrete provides thermal insulation, it offers another important advantage over conventional construction materials. Other advantages include being renewable, low impact on the environment, and obtainable from the waste stream as a by-product.

Besides the insulation property, the hemp hurd has a large capacity to absorb moisture on the internal surfaces of the plant fibers and absorb moisture in the voids of the cellular structure of the hemp. This is a desirable attribute for construction material, as it can store vapor that is driven by the interior-exterior vapor pressure difference and release it to dry when conditions change. Such a vapor storage capacity is very important in areas with high humidity, as it will not adversely affect the wall performance and durability.

### **3.2 Lime**

Natural hydraulic lime can be considered an alternative to Portland cement, when reduced carbon footprint is of interest. An example use of lime to make concrete is when it is used as the binder with lightweight aggregates, which results in a “breathable” concrete, i.e., allows vapor to pass through (Abbott 2014, Pullen 2017). However, while increasing the lime content increases the strength, it reduces the breathability, which is of interest for slab-on-grade floors.

Hydrated lime (calcium carbonate) is the binder that holds hurd (shiv) aggregates together. Over time, the carbonation process continues, which means as water is evaporated from the lime in the mixture, CO<sub>2</sub> from the air will be absorbed, which solidifies lime, as the process continues over a long time to turn the lime back to calcium carbonate. The process relies on the humidity in the air, which will be absorbed by the hemp hurd and used by the lime to continue the carbonation process. Commercial limes such as LCG mortar used in this project include some natural volcanic mineral additives to shorten the initial setting/curing time.

### **3.3 Making Hempcrete**

Bio-fiber hemp hurd is used as an aggregate, replacing gravels to make hempcrete. In addition,

hydrated lime can be used as a mineral binder to adhere hemp hurd (mulch-like shape) pieces together. Figure 10 shows the mixing of hemp hurd, lime, and water. Just as limecrete uses lime as the binder and lightweight aggregates to make lightweight concrete, hempcrete uses lime as the binder, but hemp hurd (shiv) as the aggregate, where lime basically coats the hemp shiv. The reaction between lime and water during the mixing process creates a binding property that adheres hurd particles together. Some additives can also be added to lime to control setting time, durability, and strength.



Figure 10. Mixing hemp hurd, lime and water to make hempcrete for cast in place demonstration by Americhanvre Inc.

---

Lime cures more slowly than Portland cement, but unlike Portland cement, it absorbs CO<sub>2</sub> as it sets and dries. To make concrete with lime, a volumetric mixer can measure the proportions of lime, aggregate, and water, and then an auger is used to mix the ingredients and prepare the concrete (Abbott 2014). With respect to CO<sub>2</sub> generation and absorption, it should be noted that CO<sub>2</sub> is generated and released through the process of making hydraulic lime. While CO<sub>2</sub> is generated during calcining limestone to make quick lime, once water is added to make hydrated lime, it re-absorbs 20-75% of the original CO<sub>2</sub> from the atmosphere as the concrete cures, a process known as the “lime cycle.”

Combining these facts, hempcrete is net carbon negative, e.g., the construction of a 300 mm thick hempcrete wall can be a net negative of 40 kg CO<sub>2</sub> per m<sup>2</sup> of a wall when we consider CO<sub>2</sub> absorbed during hemp growth, emission during hydrated lime production, and re-absorption by lime over time. In comparison, a masonry wall releases 100 kg of CO<sub>2</sub> emissions per m<sup>2</sup> of a wall.

### **3.4 Hempcrete Properties**

One difference between hempcrete and conventional concrete is that the voids between shiv aggregates are not necessarily filled with a lime binder, thus providing enhanced thermal insulation property (Green Home Gnome 2019). In addition, because of the porous structure of hempcrete, the breathability property of concrete made with lime is consistent with timber construction (Abbott 2014). Therefore, when the hempcrete is used for walls, it allows vapor to pass through, thus avoiding moisture accumulation that can cause many issues in walls including mold growth.

Usually, the presence of stored moisture in construction material is detrimental to its durability. In the case of hempcrete, lime with high pH coats each hemp hurd aggregate and it enhances its antimicrobial and antifungal properties. As a result, lime protects the hemp hurd from mold development under humidity and temperature conditions that can adversely affect other insulation materials. Therefore, having both high thermal insulation property and high moisture storage capacity lends this material suitable for use in home construction in both cold climates and hot and humid climates (Green Home Gnome 2017).

### **3.5 Study Plan and Method**

To establish the energy performance of the PA Hemp House, the thermal resistance properties of the walls and other surfaces need to be determined, along with the estimation of energy demand from various systems in the house. Hemp and lime material properties (density, strength, and moisture content) were determined using the information available from the product manufacturers. Indoor air conditions were determined using sensors to determine temperature, and relative humidity, which were used to evaluate indoor air quality. For energy performance evaluation, specific data was collected from the retrofitted house, drawings, and air leakage tests carried out by a third party. For such analysis, software BEopt was used, and the necessary data was collected from various sources (drawings, actual house, literature, and tests and measurements made in this study). In the following sections, details of the thermal measurement, energy analysis and indoor air quality are discussed.

---

## 4. Thermal Resistance of Walls – Heat Flow Meter Method

The Heat Flow Meter Method (HFM) (Lu and Memari 2019, 2022) is a commonly used and standardized method for in-situ measurement of building envelope assemblies. It incorporates the use of on-site installation of temperature sensors and heat flux transducers (heat flux sensors) on existing building walls whose thickness is much smaller than the other dimensions, and therefore the lateral, i.e., in-plane, heat flow can be ignored. The HFM is also based on steady-state assumption, and a certain level of a temperature difference (usually 20°C is used for steady-state measurement) between interior and exterior environments is essential. The most used calculation method for HFM is the same as that shown in Eq. (1), which is generally referred to as the “Average Model” as stated in Atsonios et al. (2017) and Deconinck and Roels (2016). However, environmental conditions can vary significantly and never reach quasi steady-state for in-situ measurement. For thermal resistance evaluation, the following aspects were followed: instrument preparation, testing protocol, testing mockup, in-situ testing, and data analysis.

### 4.1 Instruments for Thermal Resistance Measurement Study

Instruments that were employed in the hemp house thermal resistance study are as follows:

A) Six heat flux sensors (HFP01) (Figure 11): Heat-flow density or heat flow rate intensity is a measure of the flow of energy per unit area per unit time. HFP01 is a commonly used heat flux sensor that can be used to measure heat flow through soil, walls, and building envelopes. This sensor consists of a ceramics-plastic composite body that can give rise to small total thermal resistance and is expected to be a robust and stable sensor. It can be easily utilized for long-term use and in multiple locations. The uncertainty of model HFP01 is approximately  $\pm 3\%$  (Heat Flux Sensors, 2022).



Figure 11. Heat Flux Sensor HFP01 (Heat Flux Sensors, 2022).

B) 24 MF52-103/3435, 10k Ohm thermistors (Figure 12): Negative Temperature Coefficient (NTC) thermistors are small and light temperature measurement ethoxyline resin-enveloped devices with a resistance of 10K Ohm and can be used in many applications. The resistance of NTC thermistors drops as temperature increases. These thermistors are widely used for air-conditioning equipment, heating apparatus, and electric thermometers, among others (Thermistors 2022).



Figure 12. MF52-103/3435, 10k Ohm Thermistors (Thermistors 2022).

C) Three Arduino Mega2560 (Figure 13): The Arduino Mega 2560 is a microcontroller board with 54 digital input/output pins, 16 analog inputs, 4 UARTs (hardware serial ports), a 16 MHz crystal oscillator, a USB connection, a power jack, an ICSP header, and a reset button. It is simply connected to a computer with a USB cable, an AC-to-DC adapter or battery. Most shields designed for Uno, Duemilanove, and Diecimila are compatible with the Mega 2560 board (Arduino 2022).

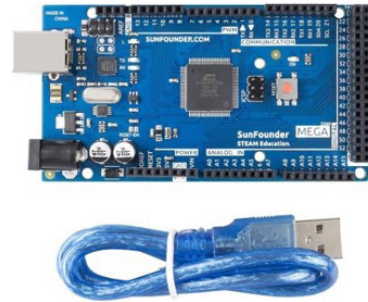


Figure 13. Arduino Mega2560 (Arduino 2022).

D) Two Analog-to-Digital Converter (ADC) (ADS1256) (Figure 14): The ADS1256 is a 24-bit analog-to-digital (A/D) converter that is very low-noise (e.g., 23-bit noise free) and can be used for high-resolution measurement solutions. The converter includes a delta-sigma ( $\Delta\Sigma$ ) modulator (4th-order) followed by a programmable digital filter (Texas Instruments 2022).

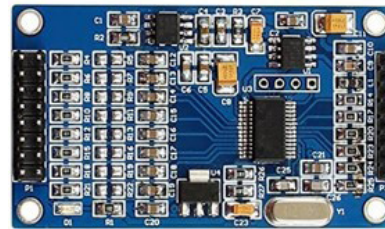


Figure 14. Analog-to-Digital Converter (ADC) (ADS1256) (Texas Instruments 2022).

E) Several Breadboards (Figure 15): A breadboard is used to develop an electronic circuit and wiring for microcontroller boards like Arduino. No soldering is needed to use this breadboard (Breadboards 2022)



Figure 15. Breadboard (Breadboards 2022).

F) Some resistors (Figure 16): As a circuit element, a resistor provides electrical resistance through two terminals. A resistor serves a wide variety of purposes in circuits, including reducing current flow and adjusting signal levels, dividing voltages, biasing active elements, and terminating transmission lines, among others (Resistors 2022).

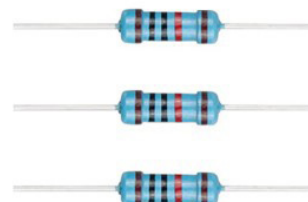


Figure 16. Electrical Resistors (Resistors 2022).

- G) Silicon heat transfer compounds (Figure 17):  
A Silicon Heat Transfer Paste is a versatile synthetic base, fortified with metal oxides, and formulated to have a paste-like consistency. It offers high thermal conductive properties, is highly resistant to heat, and is extremely stable at high temperatures (Silicon Heat Transfer 2022).



Figure 17. Silicon Heat Transfer Compound (Silicon Heat Transfer 2022).

- H) Some jumper wires and long wires (Awg22) (Figure 18): Awg20=0.81mm Diameter, Awg22=0.65mm, Awg24=0.51mm (Jumper Wires 2022).



Figure 18. Jumper Wires and Long Wires (Awg22) (Jumper Wires 2022).

## 4.2 Heat Flow Meter Methodology

At stationary conditions, the thermal resistance for the tested layer can be calculated using Eq. 1:

$$q = (T_f - T_c)/R \quad (1)$$

$q$  = density of the heat flow,  $W/m^2$

$T_f$  = temperature at the hot surface (heat flow meter),  $^{\circ}C$

$T_c$  = temperature at the cold surface,  $^{\circ}C$

$R$  = thermal resistance (R-value),  $m^2 \text{ } ^{\circ}C /W$

It is acceptable to use the method only if a)  $R$  is roughly constant, b) the heat flow direction does not change, and c) there is relatively little energy stored during the period and d) the duration of the test to be long enough (Anderlind 1992). Since the occurrence of such conditions simultaneously is not practical, other methods have been proposed.



Accordingly, a dynamic model was suggested by Anderlind (1992) as follows:

$$q_i = \frac{1}{R} (T_{i, surf, int} - T_{i, surf, ext}) + \sum_{l=1}^p A_l (T_{i-p+l, surf, int} - T_{i-p+l-1, surf, int}) + \sum_{l=1}^p B_l (T_{i-p+l, surf, ext} - T_{i-p+l-1, surf, ext}) \quad (2)$$

where  $q_i$  is the heat flux at that time ( $i^{\text{th}}$  measurement),  $T_{surf, int}$  is the interior surface temperature,  $T_{surf, ext}$  is the exterior surface temperature, and  $p$  is the number of historical data points. The constants  $A_1, \dots, A_p, B_1, \dots, B_p$  can be obtained using the regression technique over the experimental data, and  $R$  represents the thermal resistance (Lu and Memari 2018). According to Anderlind's suggestion, to get acceptable and accurate R-value results, it would be enough to measure the data for about three days (i.e., 2-day periods) (Anderlind 1992).

### 4.3 Test Setup for the Heat Flow Meter Method

Two series of experimental tests were performed on the walls of the single-family house retrofitted with hempcrete. This house was built in 1900 in New Castle, PA. Figure 19 shows the house prior to retrofit, while Figure 20 shows four photos of the exterior after the retrofit. A version of the Heat Flow Meter Method test was performed to measure the R-value of the hempcrete used in the walls in this house. Two walls of the house (after retrofit) were selected: the back wall and the sidewall of the house. Figure 21 shows the interior walls of the house with instruments attached.



Figure 19. PA Hemp House located at 506 Spruce St. New Castle, PA prior to retrofit [https://www.zillow.com/homedetails/506-Spruce-St-New-Castle-PA-16101/86510118\\_zpid/](https://www.zillow.com/homedetails/506-Spruce-St-New-Castle-PA-16101/86510118_zpid/).



Figure 20. Four different views of the Hemp House after retrofit.

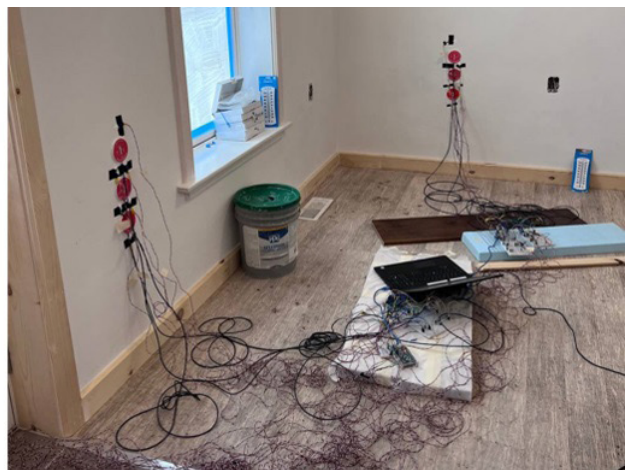
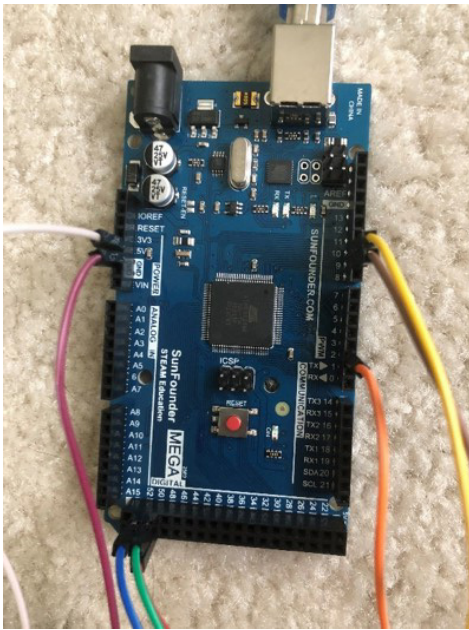


Figure 21. Positions of heat flux sensors on the side & back walls.

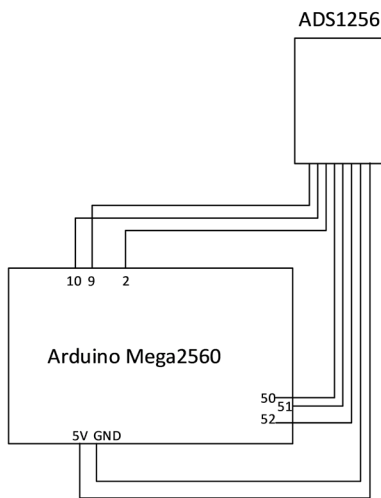
To prepare the heat flux sensors, the Arduino should be connected to the heat flux sensor using an Analog to Digital Converter (ADC). Although Arduino Mega2560 internally has an ADC, since it is rather a weak ADC, for more accurate results, using a separate ADC is recommended. Figure 22 shows how to connect the ADC1256 to Arduino mega2560. Since each Arduino has two ground (GND) pins and one 5V pin, to develop these pins, a breadboard is very useful. In such a breadboard, the pins in each row have the same properties. To have more GND and 5V pins, a connection should be between these pins in Arduino and the breadboard. Figure 22 also shows how to develop 5V and GND pins using a breadboard. For this study, an Arduino code was prepared. To connect the heat flux sensor to the Arduino according to the developed code, the connection should be as shown in Figure 23.



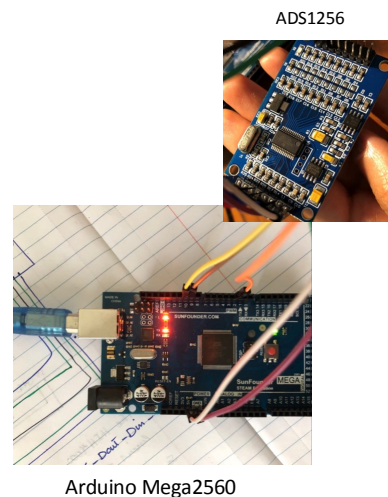
(a)



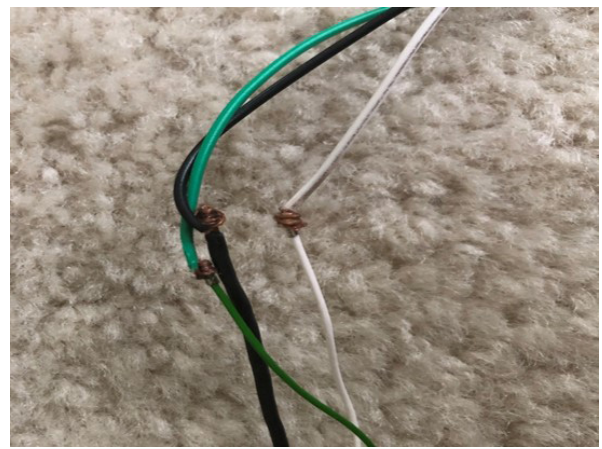
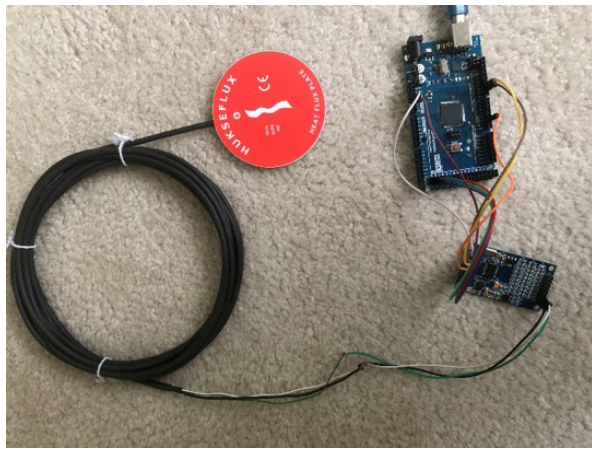
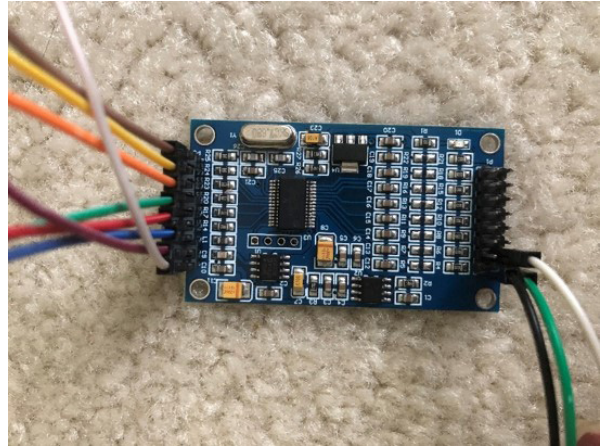
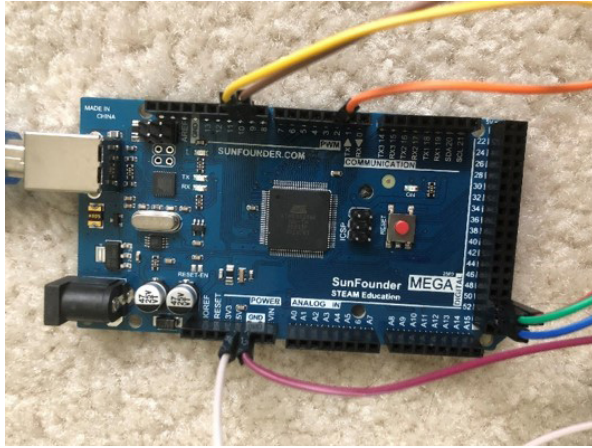
(b)



(c)



Arduino Mega2560



(d)

Figure 22. a) How the ADS1256 is connected to Arduino mega 2560, b) Arduino, c) ADC, Overall connection detail d) The connection of the heat flux sensor, Arduino, and ADC.

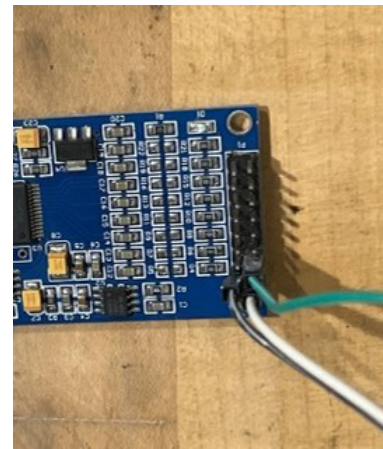


Figure 23. The connection of the heat flux to the ADC.

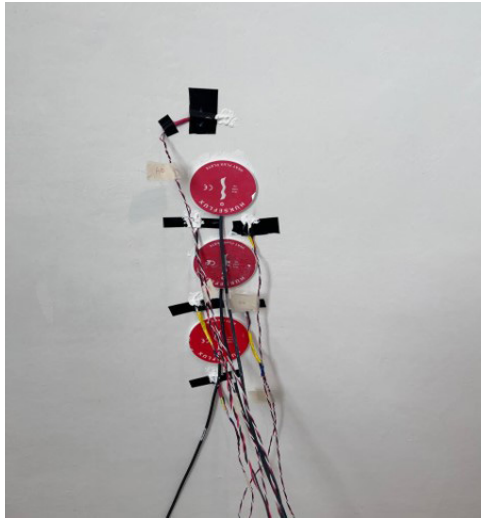
It should be noted that the heat flux data should be positive. If the heat is transferred from the environment to the room, it means that the direction of the heat transfer reverses, so the data becomes negative. The raw data obtained from the heat flux sensor is not voltage, so it should be converted to a voltage. The calculation involves the following steps:

- a) Define the ADC's reference voltage, resolution, and gain amplifier.
- b) Define the full scale of the ADC by dividing the reference voltage over the gain amplifier
- c) Define the voltage at each binary step by dividing the voltage at each binary step over the resolution.
- d) Calculate the measured voltage by multiplying the raw data obtained from the ADC to step c.
- e) Define  $q$  by dividing the measured voltage over the sensitivity of the heat flux obtained from the datasheet.

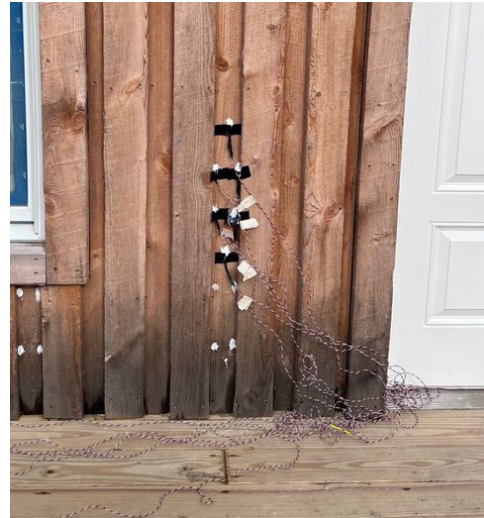
To carry out the experimental test, three heat flux sensors were mounted on the wall on the hot side (room). It is preferred to mount more than one heat flux sensor to compare the results, and by calculating the mean value of the three heat flux sensors, the results would be more reliable. Moreover, six thermistors were mounted around the heat flux sensors fully in contact with the surface of the wall to allow measuring the temperature of the surface of the wall. To do so, the heat flux sensors and thermistors were attached to the wall surface using a heat transfer compound. On the other hand, six thermistors were mounted on the cold side wall (environment/outside) at the exact opposite location of the hot side. Figures 24, 25, and 26 show the experiments set up overall and closeup.



Figure 24. Overall connection setup in the house on two walls.

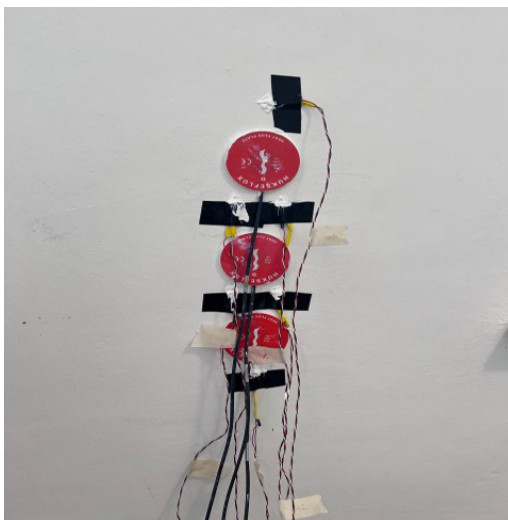


(a)

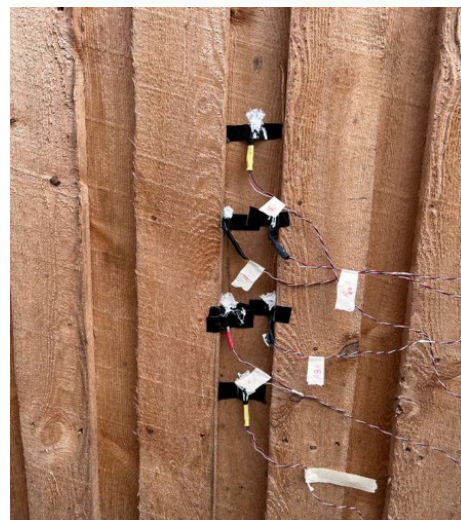


(b)

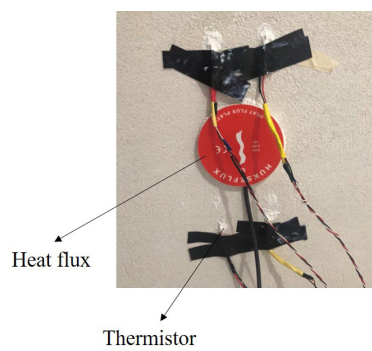
Figure 25. Sidewall set up (a) hot room set up (b) cold room set up.



(a)



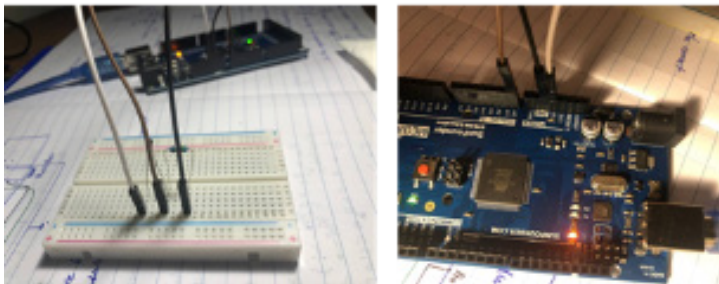
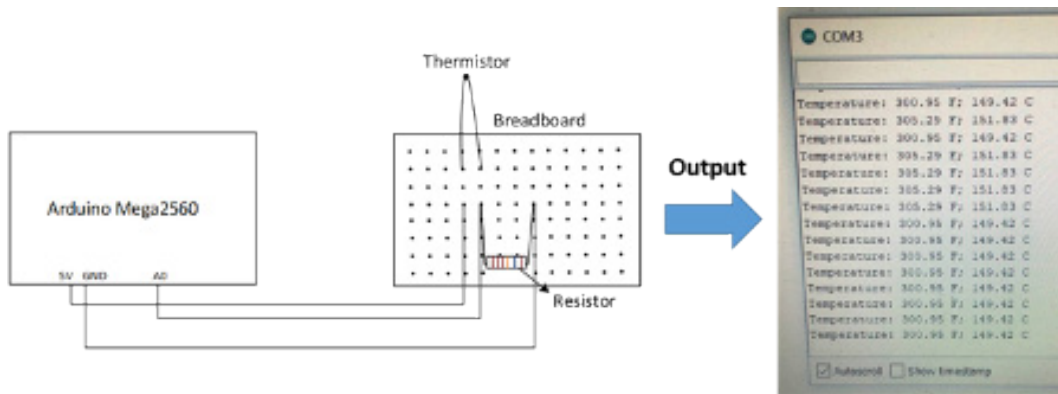
(b)



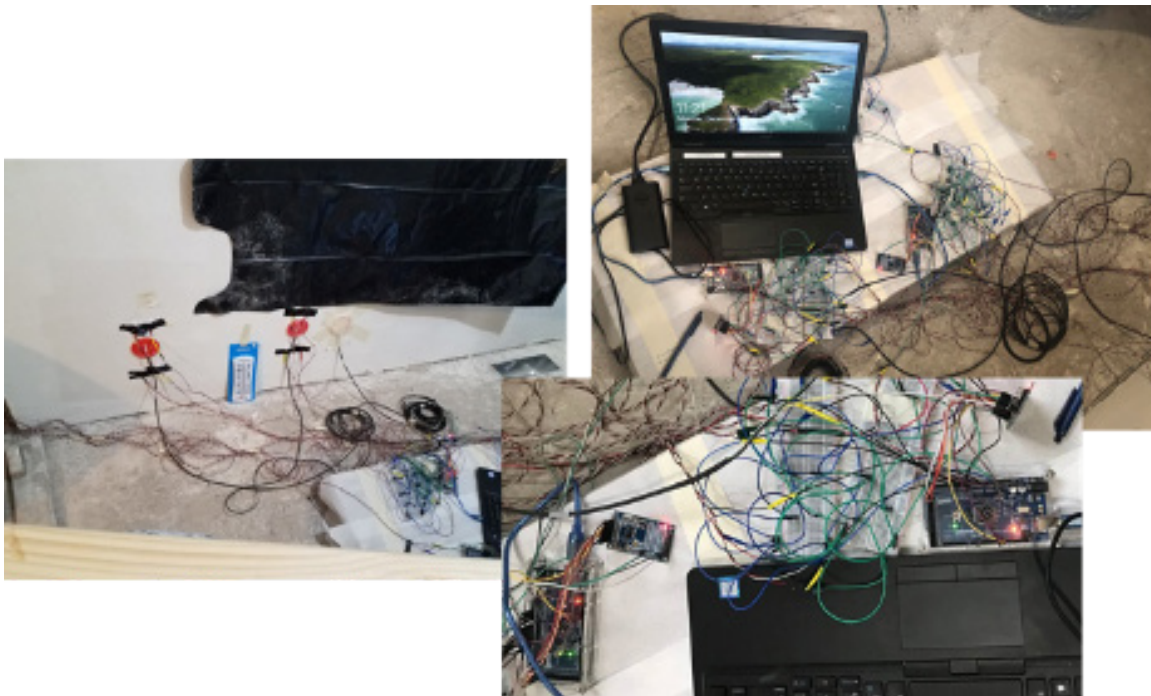
(c)

Figure 26. Back wall set up: (a) Hot room set up; (b) Cold room set up; (c) Detail.

Instruments, software, method, type of results and how to test and convert the raw data to R-value mentioned earlier are summarized in Figure 27.



(a)



(b)



(c)

Figure 27. Summary of the connections among all the sensors leading to raw data: (a) overall connection configuration; (b) Example detailed connections; (c) Research team working on the setup and making the connections.

#### 4.4 HFM Test Data and Results

The raw data obtained from the heat flux sensors should be converted to a voltage per instructions shown in Figure 28. The density of the heat flow is calculated by dividing the measured voltage by the sensitivity of the heat flux obtained from the datasheet. Also, the data obtained from the thermistors are the surface temperature on the hot and cold sides. By plugging in the values in Anderlind's formulation, the R-value is obtained.

##### Converting the raw data from heat flux sensors to q

The raw data obtained from the heat flux sensor is not voltage, so it should be converted to a voltage. The calculation involves the following steps:

- Define the ADC's reference voltage, resolution, and gain amplifier.
- Define the full scale of the ADC by dividing the reference voltage over the gain amplifier
- Define the voltage at each binary step by dividing the voltage at each binary step over the resolution.
- Calculate the measured voltage by multiplying the raw data obtained from the ADC to step c.
- Define  $q$  by dividing the measured voltage over the sensitivity of the heat flux obtained from the datasheet.

TEXAS INSTRUMENTS

ADS1255  
ADS1256

REVISION: JUNE 2015 - REVISED: SEPTEMBER 2015

### Very Low Noise, 24-Bit Analog-to-Digital Converter

**FEATURES**

- 24 Bits, No Missing Codes
  - All Data Rates and PGA Settings
- Up to 23.8 Bits/Noise-Free Resolution
- <math>-0.001\%</math> Nonlinearity (max)
- Data Output Rates to 30kSPS
  - 18.6 Bits/Noise-Free (21.3 Effective Bits) at 1.45kHz
- Fast Channel Cycling
  - 18.6 Bits/Noise-Free (21.3 Effective Bits) at 1.45kHz
- One-Shot Conversions with Single-Cycle Setting
- Flexible Input Multiplexer with Sensor Detect
  - Four Differential Inputs (ADS1255 only)
  - Eight Single-Ended Inputs (ADS1256 only)
- Chopper-Stabilized Input Buffer
- Low-Minimum-Noise (0.25-µV) Input Reference
- Self-Test
- SV<sup>2</sup>
- Ana
- Digi
- Dev

**DESCRIPTION**

The ADS1255 and ADS1256 are extremely low-noise, 24-bit analog-to-digital (A/D) converters. They provide complete high-resolution measurement solutions for the most demanding applications.

The converter is comprised of a 4th-order delta-sigma ( $\Delta\Sigma$ ) modulator followed by a programmable digital filter. A flexible input multiplexer handles differential or single-ended signals and includes circuitry to verify the integrity of the external sensor connected to the inputs. The selectable input buffer greatly increases the input impedance and the low-noise programmable gain amplifier (PGA) provides gains from 1 to 64 in binary steps.

The programmable filter allows the user to customize between a resolution of up to 23.8 bits/noise-free and a data rate of up to 50k samples per second (SPS). The converters offer fast channel cycling for measuring multiplexed inputs and can also perform one-shot conversions.

www.ti.com/ads1255

**Product certificate**

Print: 1  
Release date: 29 JUL 2021

<b>Product code</b>	<b>HF01-05</b>
<b>Product identification</b>	serial number 19172
<b>Product type</b>	heat flux plate / heat flux sensor
<b>Measured</b>	heat flux
<b>Calibration result</b>	
<b>Sensitivity</b>	$S = 57.17 \times 10^{-4} \text{ V/(W/m}^2\text{)}$
<b>Calibration uncertainty</b>	$\pm 1.72 \times 10^{-4} \text{ V/(W/m}^2\text{)}$
<p>the number following the # symbol is the expanded uncertainty with a coverage factor <math>k = 2</math>, and defines an interval estimated to have a level of confidence of 95 percent</p>	
<b>Measurement function</b>	$\Phi = U/S$ With $\Phi$ heat flux in $[\text{W/m}^2]$ , U voltage output in [V]
<b>Product specifications</b>	5 m
<b>1)</b>	cable length

Table 9-1. connections

Figure 28. Instruction for converting raw data to voltage.





---

## **5. Energy Performance Evaluation**

### **5.1 Overview**

Pre- and post-retrofit energy models were created for the hemp house to evaluate total energy use reduction. The team utilized the software program BEopt: Building Energy Optimization Tool for the energy models, which is a commonly used Graphic User Interface based on EnergyPlus simulation engine (EnergyPlus™, 2017). This software program was developed and is continuously supported and updated by the US Department of Energy and the National Renewable Energy Laboratory and is a commonly used software by researchers evaluating residential energy retrofits; the software is free to download and use by the public.

Modeling assumptions for these pre- and post-retrofit energy models were determined based on 1) a combination of pre- and post-retrofit photographs taken by team members, 2) the as-built drawing set submitted for the code review submission, 3) post-retrofit R-value measurements of the hempcrete walls, and 4) the post-retrofit blower door test report. Additionally, the post-retrofit energy model assumes the building is being used as a typical residential building (e.g., has two occupants living in the home, and uses regular appliance and laundry cycles, etc.) rather than its current use as a demonstration project (at the time of the study).

Pre-retrofit utility bills were not available for this home, and post-retrofit utility bills do not reflect a typical residential energy load profile, as there were no occupants in the home during the study period. Therefore, neither the pre- nor post-energy models were calibrated to previous pre-retrofit or current post-retrofit actual energy usage data.

Because this utility bill calibration could not be accurately performed for these energy models, it is thus important to note that the percentage differences between models will be the most accurate values rather than the absolute values shown in the tables. For example, retrofitting a home using fuel oil and a 19 ACH50 air leakage value would save any homeowner 70% on their energy bills, compared to no retrofit and assuming the same energy usage patterns pre- and post-retrofit (e.g., maintaining the same thermostat set points, etc.). However, the exact dollar amount saved will ultimately depend on that particular homeowner's usage patterns (e.g., how often they cook, how warm/cold they keep their thermostat set points, etc.). Therefore, it is most accurate to state the percentage (70% savings) rather than the absolute dollar amount (\$3,275).

Finally, eight energy models were developed for this study that varied the pre-retrofit heating and hot water fuel type and air leakage values. This approach was taken to generalize the energy and cost-saving results to reflect a wider range of housing conditions, e.g., in this neighborhood, and thus bounding anticipated percentage performance improvements if the whole-home retrofit approach utilized in this hemp house retrofit initiative were applied to other similar homes.

### **5.2 Overall Energy Modeling Approach**

To develop the pre-retrofit model, 1) pre-retrofit photos, 2) dimensions from as-built drawing sets, and 3) general assumptions based on the age and condition of the home were made. Generally, the pre-retrofit home model reflects a typical existing construction wood stud home with no insulation, no air sealing measures, single pane windows, and minimum efficiency mechanical

equipment. The models utilized TMY2 weather data from Pittsburgh International Airport, which is approximately 40 miles from the home location. Table 2 shows the basic pre- and post-retrofit home characteristics for this energy modeling study. Figure 30 shows the BEopt model for the house.

Table 2. Pre- and Post-Retrofit Home Characteristics.

	<b>Pre-Retrofit</b>	<b>Post-Retrofit</b>
Walls	Uninsulated	Insulated (R-17)
Roof	Uninsulated	Insulated (R-38)
Basement Ceiling (1/2 of house)	Uninsulated	Insulated (R-19)
Slab (1/2 of house)	Uninsulated	Uninsulated
Windows	Single Pane (U-0.84)	Double Pane (U-0.30)
Air sealing	No air sealing (10-19 ACH50)	Code-level air sealing (4.96 ACH50)
Heating system	Furnace (78% Annual Fuel Utilization Efficiency)	Heat Pump, ducted (8.2 Heating Season Performance Factor)
Cooling system	Window A/C units (8.5 Energy Efficiency Rating)	Heat Pump, ducted (16 Seasonal Energy Efficiency Rating)
Water Heating System	Tanked, Standard Efficiency (0.62 EF)	Electric Tank, Standard Efficiency (0.92 EF)



Figure 30. Graphical representation of the home in BEopt. Note: BEopt requests total window area per façade and total door area rather than asking for size and location of specific windows and doors. Therefore, the graphical representation shown does not show windows and doors in the exact location as the actual hemp house.

A goal for the energy modeling portion of the work was to generalize the results to reflect a wider range of housing conditions, e.g., in this neighborhood. Therefore, for this study, eight energy models (Table 3) were created that changed the pre-retrofit heating and hot water fuel types and the pre-retrofit airtightness levels.

Table 3. Models Considered for BEopt Analysis.

	10 ACH50	13 ACH50	16 ACH50	19 ACH50
<b>Natural Gas</b> - 78% Annual Fuel Utilization Efficiency (AFUE) Natural Gas Furnace - 40-Gal Natural Gas Standard Water Heater, 0.62 Energy Factor (EF)	<i>Model #1</i>	<i>Model #2</i>	<i>Model #3</i>	<i>Model #4</i>
<b>Fuel Oil</b> - 78% AFUE Fuel Oil Furnace - 40-Gal Fuel Oil Standard Water Heater, 0.62 Energy Factor (EF)	<i>Model #5</i>	<i>Model #6</i>	<i>Model #7</i>	<i>Model #8</i>

### 5.3 Wall Modeling Approach

The post-retrofit hempcrete wall is similar in structure and materials to a double wood stud wall construction type. See Figure 31 below for the full post-retrofit wall assembly details.

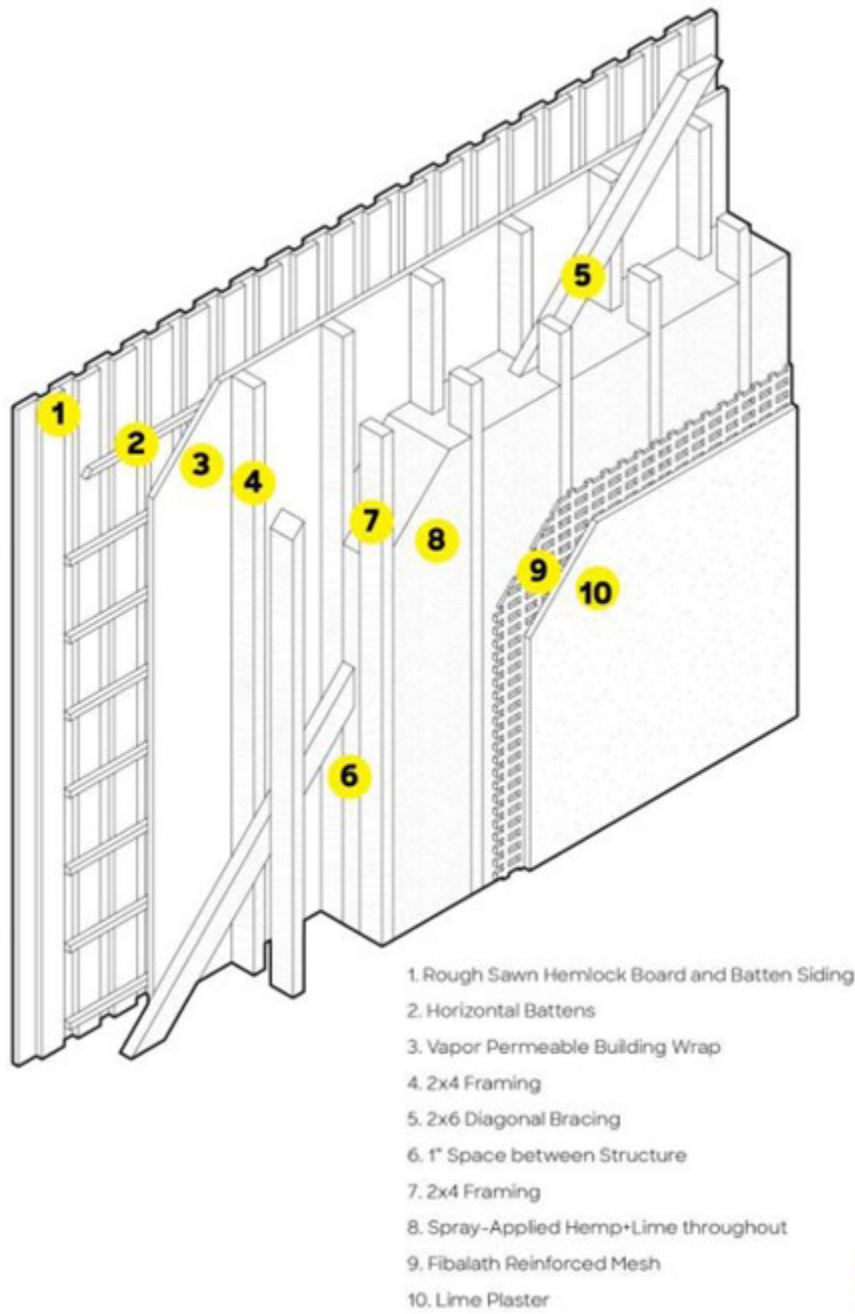


Figure 31. Post-retrofit hempcrete wall.

To work within the parameters of BEopt’s retrofit interface, the pre- and post-retrofit walls were modeled in two ways, as shown in Table 4.

Table 4. Wall Modeling Assumptions for BEopt Analysis.

	<b>Wall Modeling Method #1</b>	<b>Wall Modeling Method #2</b>
<b>Pre-Retrofit Wall</b>	Uninsulated double stud wall (R-4.4 overall assembly R-value)	Uninsulated 2x6 wood stud wall (R-4.1 overall assembly R-value)
<b>Post-Retrofit Wall</b>	Uninsulated double stud wall (R-4.4) with a R-12.6 continuous insulation layer to achieve a total overall assembly R-value of R-17	Insulated 2x6 wood stud wall with R-19 cavity insulation (R-16.8 overall assembly R-value)

These modeling approaches were taken for several reasons:

- BEopt’s retrofit interface currently reflects standard wall retrofit practices, e.g., the addition of insulation into wood stud cavity walls, the addition of an exterior continuous insulation layer, etc. Thus, BEopt’s retrofit interface does not currently provide options to modify a pre-retrofit single-stud wall to be a post-retrofit double-stud wall.
- Additionally, BEopt did not permit custom component development of a post-retrofit double-stud wall with added cavity insulation.

Therefore, these two approaches aim to reflect the total wall assembly R-value that was measured on site (R-17), while also accounting for the balance of wood vs. insulation materials physically present in the pre- and post-retrofit walls.

Ultimately the results of Wall Modeling Method #1 are reflected in this report, as this method yielded more conservative energy savings (Wall Modeling Method #2 yielded approximately 2% greater projected energy savings.)

#### **5.4 Energy Modeling and Analysis Results**

The energy modeling results showed an approximately 75% reduction in total site energy usage between the pre- and post-retrofit home energy models (Figure 32). Table 5 shows the breakdown of pre- and post-retrofit energy usage in million British Thermal Units (MMBTU) for each model (i.e., each combination of pre-retrofit heating and hot water fuel type and pre-retrofit airtightness). The significant site energy savings reflects the whole-home retrofit approach utilized in the hemp house project to systematically improve the building envelope (insulation, air sealing, and windows) and installing significantly higher efficiency heating and cooling systems (i.e., furnace to heat pump conversion).

Table 5. Total Energy Usage Reductions (MMBTU).

Pre-Retrofit Heating Fuel Type	Pre-Retrofit Airtightness	Model #	Pre-Retrofit Total Site Energy Use (MMBTU)	Post-Retrofit Total Site Energy Use (MMBTU)	Difference (MMBTU)	% Difference
Natural Gas	10 ACH50	Model #1	141.8	37.0	-104.8	-74%
	13 ACH50	Model #2	148.3		-111.3	-75%
	16 ACH50	Model #3	154.8		-117.8	-76%
	19 ACH50	Model #4	161.4		-124.4	-77%
Fuel Oil	10 ACH50	Model #5	141.1	37.0	-104.1	-74%
	13 ACH50	Model #6	147.6		-110.6	-75%
	16 ACH50	Model #7	154.1		-117.1	-76%
	19 ACH50	Model #8	160.8		-123.8	-77%

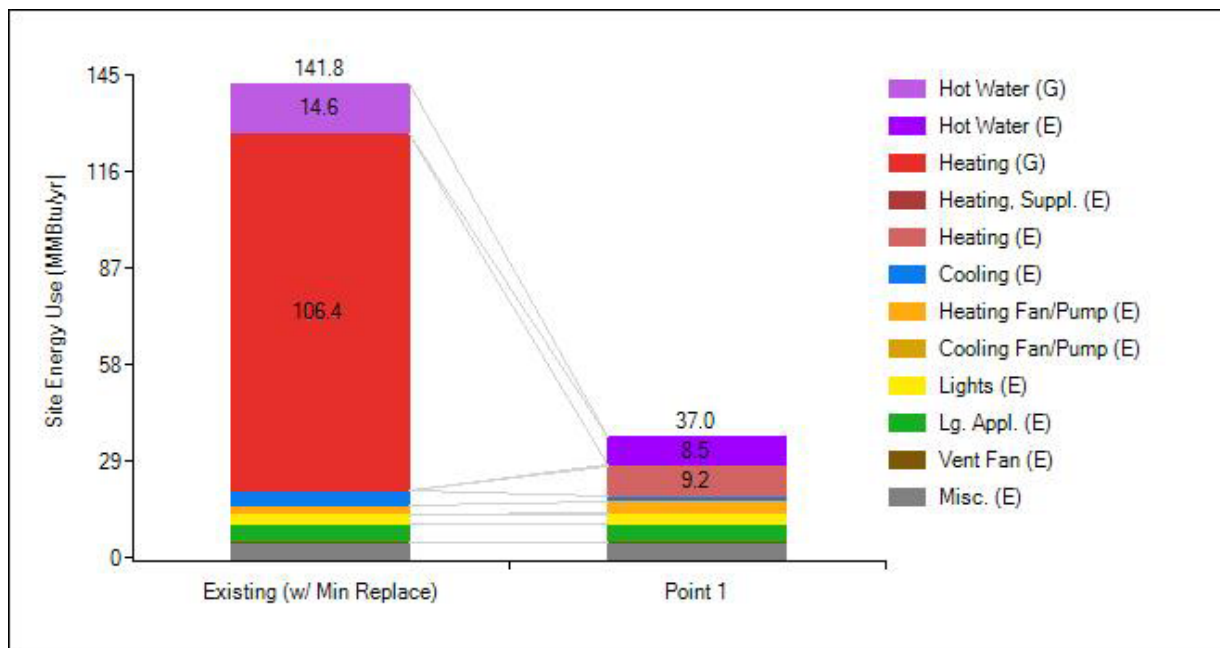


Figure 32. Pre- and Post-Retrofit BEopt graph of Site Energy Usage (MMBTU/year) for Model #1.

Given the conversion of the home from one using multiple fuel types (i.e., natural gas or fuel oil for heating and hot water and electricity for all other systems) to one using a single fuel type (i.e., electricity for all systems), the energy use reductions by fuel type were evaluated for each model. Tables 6 and 7 and Figures 33 and 34 show the breakdown by energy model in kilowatt-hours (electricity) and either therms of natural gas or gallons of fuel oil. A positive value indicates an increase in use of that fuel type, while a negative value indicates a reduction in the use of that fuel type. For this retrofit, the hemp house retrofit utilized all-electric systems, and therefore all post-retrofit energy models show a 100% reduction (-100%) in natural gas or fuel oil usage and a corresponding increase (+73% to +78%) of electricity usage for heating and hot water.

Table 6. Energy Usage Reductions for Natural Gas Homes.

Model #	Pre-Retrofit Electricity Usage (kWh)	Post-Retrofit Electricity Usage (kWh)	Diff. (kWh)	% Diff.	Pre-Retrofit Natural Gas Usage (Therms)	Post-Retrofit Natural Gas Usage (Therms)	Diff. (Therms)	% Diff.
Model #1	6,104	10,851	+4,747	+78%	1,209	0	-1,209	-100%
Model #2	6,166		+4,685	+76%	1,272		-1,272	-100%
Model #3	6,225		+4,626	+74%	1,336		-1,336	-100%
Model #4	6,286		+4,565	+73%	1,400		-1,400	-100%

Table 7. Energy Usage Reductions for Fuel Oil Homes.

Model #	Pre-Retrofit Electricity Usage (kWh)	Post-Retrofit Electricity Usage (kWh)	Difference (kWh)	% Diff.	Pre-Retrofit Fuel Oil Usage (Gallons)	Post-Retrofit Fuel Oil Usage (Gallons)	Diff. (Gallons)	% Diff.
Model #5	6,103	10,851	+4,748	+78%	865	0	-865	-100%
Model #6	6,163		+4,688	+76%	911		-911	-100%
Model #7	6,223		+4,628	+74%	956		-956	-100%
Model #8	6,285		+4,566	+73%	1,003		-1,003	-100%

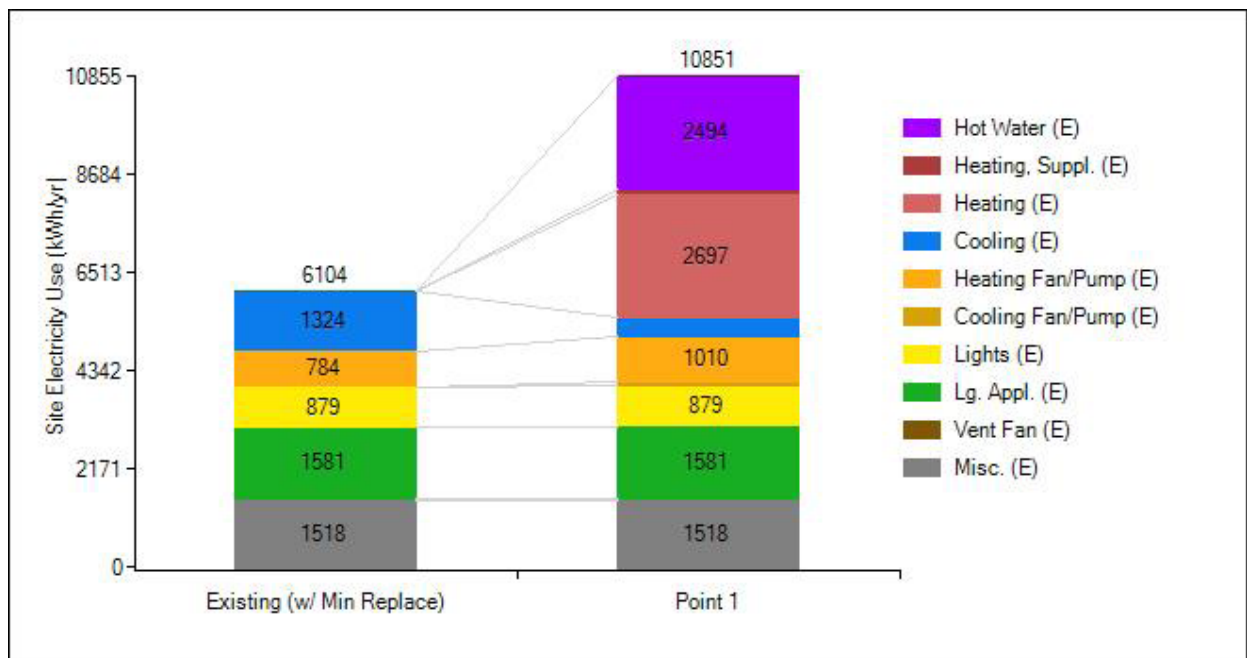


Figure 33. Pre- and Post-Retrofit BEopt graph of Site Electricity Usage (kWh/year) for Model #1.



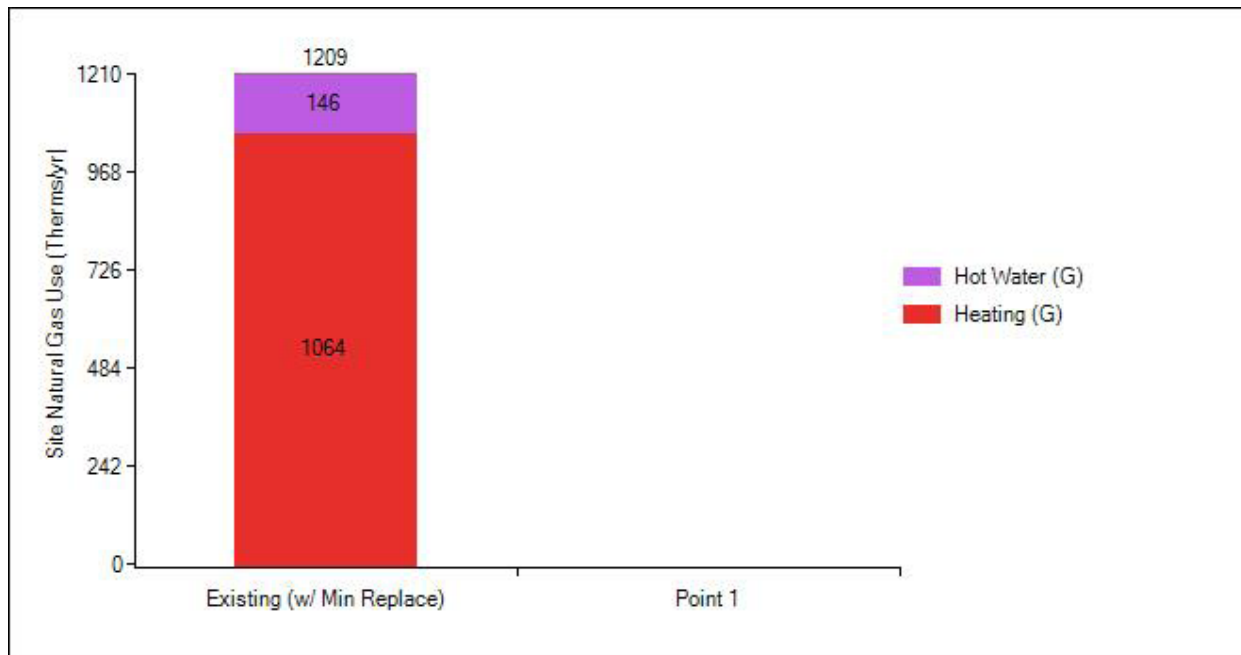


Figure 34. Pre- and Post-Retrofit BEopt graph of Site Natural Gas Usage (Therms/year) for Model #1.

## 5.5 Energy Cost Results

To evaluate impacts on energy costs, the unit costs per fuel type shown in Table 8 were utilized in this study. Unit cost values reflect the latest published data by the Energy Information Agency (EIA) for each fuel type for a cite as close to the project location as possible (New Castle, PA).

Table 8. Fuel Costs Assumptions.

Fuel Type	Unit Cost	Source	Link
Electricity	\$0.1276 / kWh	2020 average retail price for Penn Power residential customers	<a href="http://www.eia.gov/electricity/sales_revenue_price/pdf/table6.pdf">www.eia.gov/electricity/sales_revenue_price/pdf/table6.pdf</a>
Natural Gas	\$1.11 / therm	2020 average retail price for Pennsylvania customers	<a href="http://www.eia.gov/dnav/ng/ng_pri_sum_a_EPG0_PRS_DMcf_a.htm">www.eia.gov/dnav/ng/ng_pri_sum_a_EPG0_PRS_DMcf_a.htm</a>
Fuel Oil	\$3.85 / gallon	October 2021-March 2022 average retail price for Central Atlantic customers	<a href="http://www.eia.gov/dnav/pet/pet_pri_wfr_a_EPD2F_PRS_dpgal_m.htm">www.eia.gov/dnav/pet/pet_pri_wfr_a_EPD2F_PRS_dpgal_m.htm</a>

Evaluation of the energy cost reductions for the retrofitted house showed a 35-41% reduction in energy costs compared to the same home assumed using natural gas as its heating and hot water fuel source, and a 66-70% reduction in energy costs compared to the home if assumed using fuel oil as its heating and hot water fuel source.

Tables 9 and 10 show the total energy cost reductions, as well as the cost savings breakdown by

fuel type. For example, Model #1, a house using natural gas for heating and hot water and with a 10 ACH50 air leakage value, is projected to cost a homeowner \$2,117 to operate pre-retrofit and \$1,385 post-retrofit, resulting in 35% in total energy savings (see note in the Overview section regarding the interpretation of dollar vs. percentage results for this study). For comparison, Model #5 that is the same house but uses fuel oil for heating and hot water, projected to cost a homeowner \$4,109 to operate pre-retrofit and \$1,385 post-retrofit, resulting in 66% in total energy savings. The energy cost savings breakdown in Tables 9 and 10 show the breakdown of energy bill costs by fuel type, with the pre-retrofit natural gas and fuel oil costs constituting the largest percentage of the home fuel costs.

Table 9. Total Energy Cost Savings (\$).

Pre-Retrofit Heating Fuel Type	Pre-Retrofit Airtightness	Model #	Pre-Retrofit Total Energy Cost (\$)	Post-Retrofit Total Energy Cost (\$)	Diff. (\$)	% Diff.
Natural Gas	10 ACH50	Model #1	\$2,117	\$1,385	-\$733	-35%
	13 ACH50	Model #2	\$2,195		-\$810	-37%
	16 ACH50	Model #3	\$2,273		-\$888	-39%
	19 ACH50	Model #4	\$2,352		-\$967	-41%
Fuel Oil	10 ACH50	Model #5	\$4,109	\$1,385	-\$2,724	-66%
	13 ACH50	Model #6	\$4,290		-\$2,906	-68%
	16 ACH50	Model #7	\$4,474		-\$3,089	-69%
	19 ACH50	Model #8	\$4,661		-\$3,277	-70%

Table 10. Energy Cost Savings Breakdown by Electricity and Natural Gas.

Model #	Pre-Retrofit Electricity Cost (\$)	Post-Retrofit Electricity Cost (\$)	Diff. (\$)	% Diff.	Pre-Retrofit Natural Gas Cost (\$)	Post-Retrofit Natural Gas Cost (\$)	Diff. (\$)	% Diff.
Model #1	\$779	\$1,385	+\$606	+78%	\$1,338	\$0	-\$1,338	-100%
Model #2	\$787		+\$598	+76%	\$1,408		-\$1,408	-100%
Model #3	\$794		+\$590	+75%	\$1,479		-\$1,479	-100%
Model #4	\$802		+\$583	+73%	\$1,550		-\$1,550	-100%

Table 11. Energy Cost Savings Breakdown by Electricity and Fuel Oil.

Model #	Pre-Retrofit Electricity Cost (\$)	Post-Retrofit Electricity Cost (\$)	Diff. (\$)	% Diff.	Pre-Retrofit Fuel Oil Cost (\$)	Post-Retrofit Fuel Oil Cost (\$)	Diff. (\$)	% Diff.
Model #5	\$779	\$1,385	+\$606	+78%	\$3,330	\$0	-\$3,330	-100%
Model #6	\$787		+\$598	+76%	\$3,504		-\$3,504	-100%
Model #7	\$794		+\$593	+74%	\$3,680		-\$3,680	-100%
Model #8	\$802		+\$583	+73%	\$3,859		-\$3,859	-100%

---

## 6. Indoor Environmental Quality (IEQ) Study

A remote monitoring station was used to collect indoor environmental quality data. We used an Onset HOBO RX3000 base station to collect data via cellular and then store data in the cloud-based HOBOLink system (Figure 35). The data collected includes indoor air temperature, relative humidity, and carbon dioxide (CO<sub>2</sub>) concentration. All sensors were Onset except for the Telaire CO<sub>2</sub> monitor, as it was the only one compatible with the RX3000 system. Additionally, a moisture sensor was embedded in the exterior hempcrete wall to monitor any changes to the moisture content of the hempcrete. All sensors were deployed in early April 2022, while construction was still on-going through mid-September 2022. A combined air temperature and relative humidity sensor was installed in the living space on the ground floor, and another was in the bedroom on the upper floor. The CO<sub>2</sub> sensor was also located in the living space on the ground floor. The moisture sensor was embedded approximately halfway into the depth of the hempcrete wall in the upstairs bathroom. This location was selected both due to the ease of installing the sensor in the hempcrete in this location, access to a window to power the solar cells on the sensor, and if possible, to understand the impact of typical bathroom-related moisture on the hempcrete.

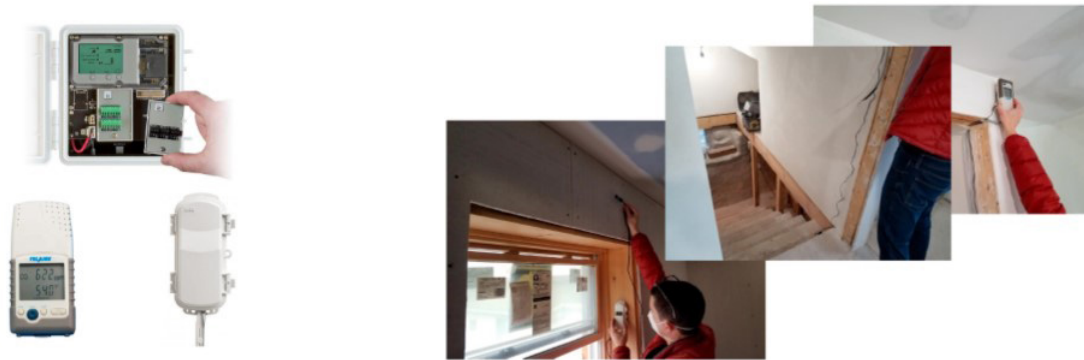


Figure 35. Images of the base station and sensors used in this project. Photographs of the sensor locations, including moisture content (left) and CO<sub>2</sub> (right). The data collection hub was deployed in a storage space adjacent to the basement stairs (center).

Air temperature and relative humidity are two primary indicators for thermal comfort. The American Society of Heating, Refrigerating, and Air-Conditioning Engineers (ASHRAE) Standard 55 states that acceptable indoor air temperatures could range between 67°F and 82°F and recommends temperatures of 68°F to 74°F in the winter and 72°F to 80°F in the summer. ASHRAE Standard 62.1 recommends that relative humidity in occupied spaces should be held below 65% to reduce the likelihood of conditions that could lead to mold and mildew growth. Relative humidity of 30% to 60% is recommended because a low relative humidity (less than 30%) can cause eye irritation, stuffy nose, aggregate allergies, and increase the spread of viral infections.

Carbon dioxide concentration measured in parts per million (ppm) is used to assess air quality and is often used as a proxy for ventilation rates. Higher indoor CO<sub>2</sub> concentrations are associated with impaired cognitive function, increased health symptoms, and perceived poor air quality. Higher indoor CO<sub>2</sub> concentrations are also associated with less ventilation and less fresh outdoor air. Carbon dioxide concentrations can also be used to understand how spaces are

occupied as more people will generate more CO<sub>2</sub>. ASHRAE Standard 62 recommends keeping indoor CO<sub>2</sub> concentrations below 1,000 ppm to avoid the negative impacts outlined above.

The indoor air temperature profiles for the house during typical weeks in June and August 2022 (Figure 36) show that the house, with the assistance of its HVAC system, kept the ground floor and upstairs spaces within the ranges suggested by ASHRAE except for overcooling in the evenings in June.

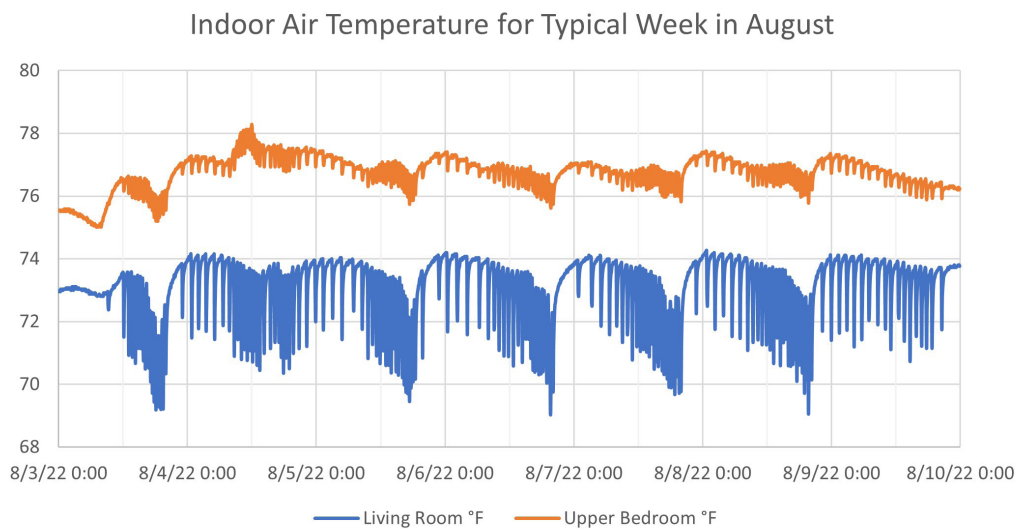
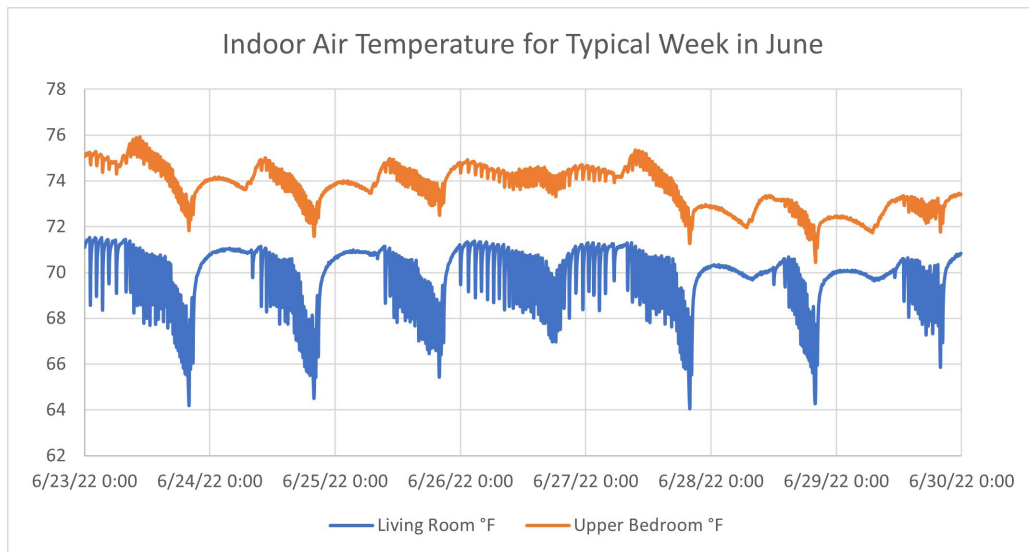


Figure 36. Indoor air temperature profiles during typical weeks in June and August 2022.

On a hotter than average day in June, such as June 22, the cooling cycle of the HVAC system can be seen in the abrupt two-degree air temperature dips throughout the day and evening. On a more average June day, there is no mechanical cooling needed between 9 pm and 8 am. A consistent indoor temperature overnight can be seen in the June 24 graph below (Figure 37).

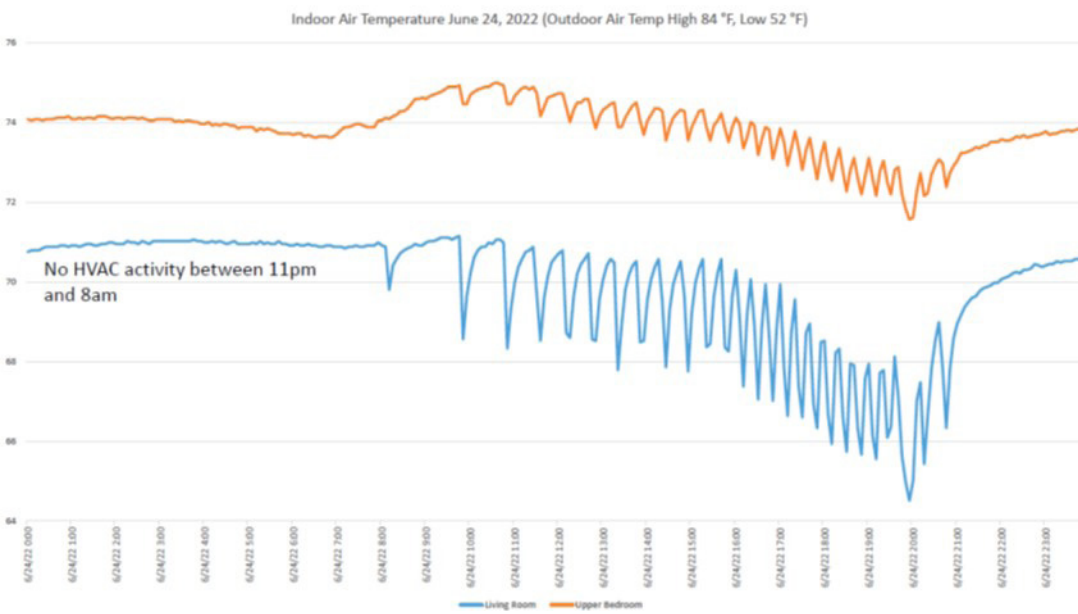
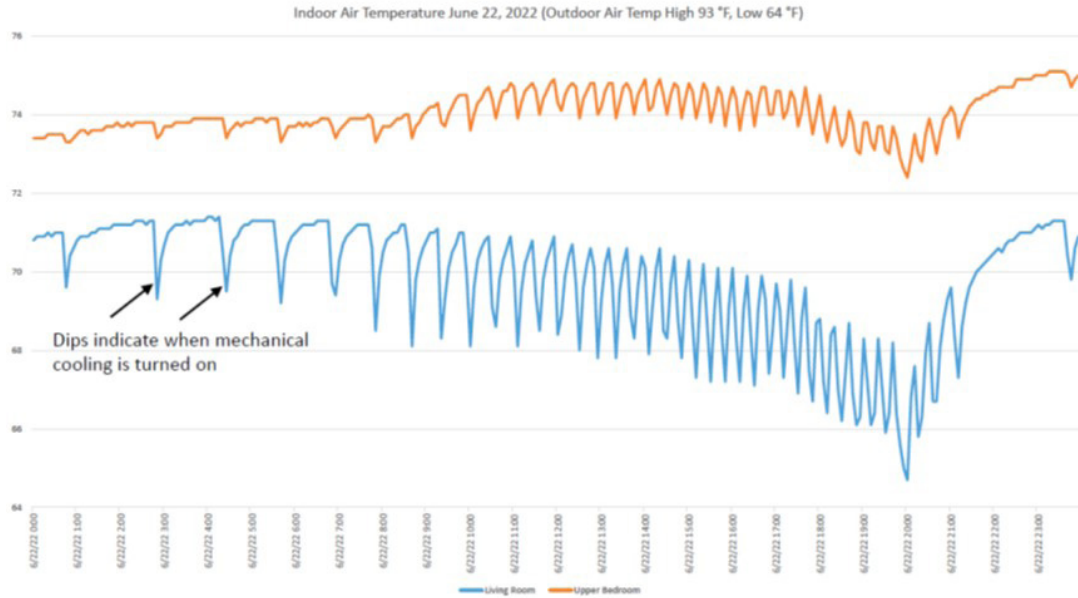


Figure 37. Consistent indoor temperature overnight during June 24, 2022.

On a cooler than average day in August, the air temperature data collected (Figure 38) suggests that the HVAC system did not operate (or at least it did not provide any heating or cooling). The relatively even temperature distribution throughout the day (with only a 1.5°F change in temperature in either space) demonstrates the high insulative properties of the hempcrete walls as well as the thermal mass they provide. Without the hempcrete, we would expect higher temperature swings indoors, even on a mild day. The steeper increase in air temperature in the upper bedroom starting at 8am is likely due to direct sunlight penetrating the upstairs bedroom windows.

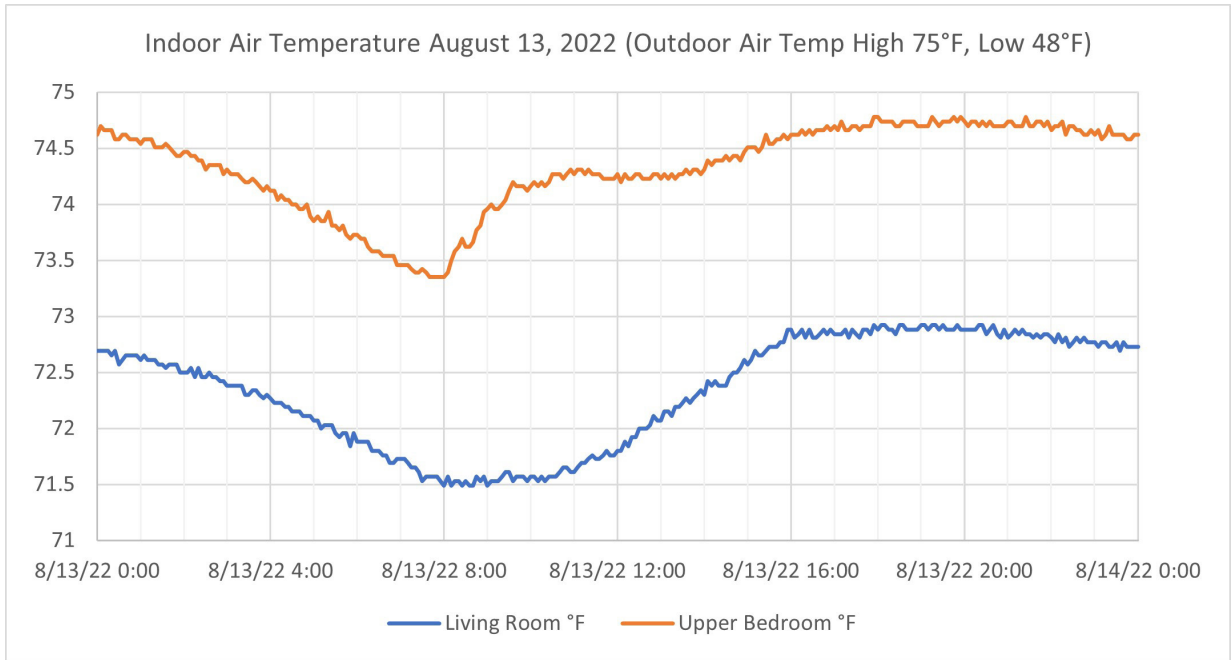


Figure 38. Indoor Air Temperature during August 13, 2022.

Despite high outdoor humidity levels during hot summer weeks, the indoor relative humidity (Figure 39) was always less than 60%, with an average relative humidity range between 44% and 52%. This demonstrates the ability of the hempcrete to moderate the indoor humidity levels to both prevent the growth of mold as well as avoid low indoor humidity levels that may cause respiratory irritation and increase the spread of airborne disease.

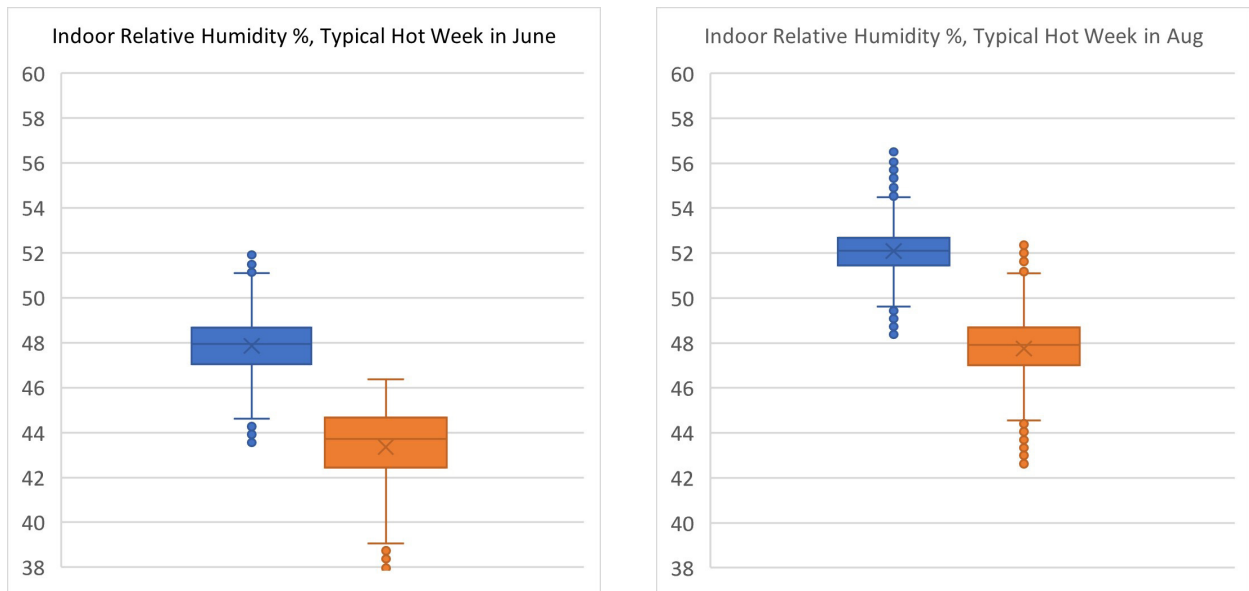


Figure 39. Indoor Relative Humidity.

---

As the house was largely unoccupied, the CO<sub>2</sub> levels (Figure 40) remained below the 1,000 PPM threshold throughout the monitoring period. Even during the end of construction in April, the CO<sub>2</sub> levels rarely went above 1,000 PPM and only for very short periods of time. Again, these findings confirm that the hempcrete walls in combination with the HVAC system help maintain indoor air quality parameters associated with healthy outcomes.

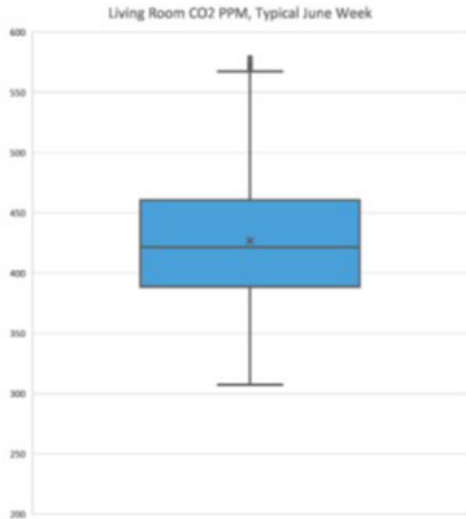


Figure 40. Living Room CO2 Level.

When the moisture content sensor was deployed in April 2022, the hempcrete was already very dry, as it had been placed months earlier. Consequently, the volumetric water content was at 10% on April 8, 2022, and went down to 9% by the end of May and stayed at 9% throughout the summer with very slight fluctuations within the margin of error of the sensor. In a future study, inserting the moisture content sensor when the hempcrete is being placed would lead to a better understanding of the drying process. As the house was largely unoccupied during the summer, the hypothesis that moisture from normal bathroom use might impact the hempcrete was not tested.

---

## 7. Summary and Conclusions

The study presented focused on instrumentally determining thermal properties of the walls and indoor air quality and evaluating energy performance through simulation for a home in New Castle, PA retrofitted using hempcrete. The main objectives of the study were determination of hempcrete walls' thermal insulative properties and the resulting impact on utility costs and indoor air quality. The approach used to determine thermal properties included Heat Flow Meter Method that led to determination of the whole wall R-value.

The effect of using hempcrete on energy consumption was determined through energy modeling of the house based on the software BEopt. To illustrate the effect of using hempcrete as the main insulation type in the wall, a comparison was made with the case of the house prior to retrofit, where the walls did not have insulation, and a comparison with the energy consumption assuming the house was retrofitted following the conventional batt insulation solution.

Another aspect of the study was to evaluate the indoor air quality after the construction was completed. Accordingly, instruments consisting of thermometers, humidity sensors, and CO<sub>2</sub> sensors were mounted inside the house to read the parameters of interest and provide readings over a period of several months.

To establish the energy performance, the thermal resistance properties of the walls and other surfaces were determined instrumentally or assumed based on literature review. Hemp and lime material properties (density, strength, and moisture content) were determined using the information available from the product manufacturers. Indoor air conditions were determined using sensors to determine temperature, and relative humidity, which were used to evaluate indoor air quality. For energy performance evaluation, specific data was collected from the retrofitted house, drawings, literature, and air leakage tests carried out by a third party. Such data was used in BEopt modeling to determine energy savings compared to the original conditions of the house.

The study led to the following conclusions:

1. The measured R-value for the whole wall turned out to be approximately R-17. The sensors for the study were mounted on both sides of the wall consisting of (interior to exterior)  $\frac{3}{4}$  in. hemp rich plaster, 10 in. thick hempcrete,  $\frac{1}{2}$  in. air space, and  $\frac{1}{2}$  in. thick rough sawn hemlock board siding.
2. The energy modeling results showed an approximately 75% reduction in total site energy usage between the pre- and post-retrofit home energy models
3. The significant site energy savings shows that using hempcrete as the wall insulation and installing high efficiency HVAC system improves the building envelope performance.
4. The study shows that retrofitted house has a 35-41% reduction in energy costs compared to the same home assumed using natural gas as its heating and hot water fuel source, and a 66%-70% reduction in energy costs compared to the home if assumed using fuel oil as its heating and hot water fuel source.
5. The indoor air temperature profiles for the house during typical weeks in June and August 2022 show that the house, with the assistance of its HVAC system, kept the ground floor



---

and upstairs spaces within the ranges suggested by ASHRAE, except for overcooling in the evenings in June. On a more average June day, there is no mechanical cooling needed between 9 p.m. and 8 a.m.

6. The relatively even temperature distribution (i.e., no indoor temperature swing) throughout the day in August demonstrates the high insulative properties of the hempcrete walls as well as the thermal mass they provide.
7. Despite high outdoor humidity levels during hot summer weeks, the indoor relative humidity was always less than 60%, which demonstrates the ability of the hempcrete to moderate the indoor humidity levels. This will both prevent the growth of mold as well as avoid low indoor humidity levels that may cause respiratory irritation and increase the spread of airborne disease.
8. As the house was largely unoccupied, the CO<sub>2</sub> levels remained below the 1,000 PPM threshold throughout the monitoring period. This finding confirms that the hempcrete walls in combination with the HVAC system help maintain indoor air quality parameters associated with healthy metrics.

The results of this effort can be used in follow-up studies toward development of standards, which can be incorporated in the building code in the future.

---

## References

- Abbott, T., (2014). "Limecrete FAQ," The Limecrete Company LTD Sustainable Construction. <http://limecrete.co.uk/limecrete-faq/>.
- Anderlind, G., (1992). 'Multiple Regression Analysis of Thermal Measurements—Study of an Attic Insulated with 800 mm Loose', Journal of Building Physics. doi: doi.org/10.1177/109719639201600109.
- Architecture 2030, (2022). "Why the Built Environment?" <https://architecture2030.org/why-the-building-sector/#:~:text=The%20built%20environment%20generates%20nearly,for%20an%20additional%2020%25%20annually>, (accessed 09/11/22).
- Arduino Mega, (2022). Available Online: <https://store-usa.arduino.cc/products/arduino-mega-2560-rev3>; (Site visited 5/19/2022).
- Atsonios, I. A. et al., (2017). "A comparative assessment of the standardized methods for the in-situ measurement of the thermal resistance of building walls," Energy and Buildings. Elsevier B.V., 154, pp. 198–206. doi: 10.1016/j.enbuild.2017.08.064.
- Breadboard, (2022). Available Online: <https://www.seeedstudio.com/blog/2020/01/06/how-to-use-a-breadboard-wiring-circuit-and-arduino-interfacing/>; (Site visited 5/19/2022).
- Deconinck, A. H. and Roels, S., (2016). "Comparison of characterisation methods determining the thermal resistance of building components from onsite measurements,' Energy and Buildings. Elsevier B.V., 130, pp. 309–320. doi: 10.1016/j.enbuild.2016.08.061.
- EnergyPlus™, (2017). Computer software. <https://www.osti.gov/servlets/purl/1395882>. Vers. 00. USDOE Office of Energy Efficiency and Renewable Energy (EERE), Energy Efficiency Office. Building Technologies Office. 30 Sep. 2017.
- Global Alliance for Buildings and Construction (GABC), (2019). "2019 Global Status Report for Buildings and Construction – Towards a zero-emissions, efficient and resilient buildings and construction sector," UN Environment Programs, International Energy Agency, ISBN No.: 978-92-807-3768-4.
- Green Home Gnome (GHG), (2017). "6 Advantages of Building with Hempcrete," <https://www.greenhomegnome.com/advantages-building-hempcrete/> (site visited May 2022).
- GreenSpec, (2019). "Tradical Hempcrete -- Bio-composite Building Material," <http://www.greenspec.co.uk/green-products/in-situ-composites/details/tradical-hempcrete/>; (site visited May 2022).
- Heat Flux Sensors, (2022). Available Online: <https://www.hukseflux.com/products/heat-flux-sensors/heat-flux-meters/hfp01-heat-flux-sensor>; (Site visited 5/19/2022).

---

Hobo Link System, (2022). "HOBOLink Web-Based Display/Readout," <https://www.onsetcomp.com/products/software/hobolink/>, (Site visited 3/10/2022).

Jumper Wires, (2022). "Premium Female/Male 'Extension' Jumper Wires," [https://www.adafruit.com/product/1953?gclid=CjwKCAjwKmaBhBMEiwAyINuWA-oleOWcEsP9EPTehY9VSjxbcNmG-o5dhIYbyAmvI79r02WIZaJBxoCgBsQAvD\\_BwE](https://www.adafruit.com/product/1953?gclid=CjwKCAjwKmaBhBMEiwAyINuWA-oleOWcEsP9EPTehY9VSjxbcNmG-o5dhIYbyAmvI79r02WIZaJBxoCgBsQAvD_BwE), (Site visited 5/19/2022).

Lu, X., and Memari, A. M. (2018)., "Comparative Study of Hot Box Test Method Using Laboratory Evaluation of Thermal Properties of a Given Building Envelope System Type." *Energy Build.*, 178, 130–139.

Lu, X. and Memari, A. M., (2019). "Determination of Exterior Convective Heat Transfer Coefficient for Low-Rise Residential Buildings," to Submitted to Taylor and Francis *Journal of Advances in Building Energy Research*, Published online May 6, 2019; 19 p, DOI: 10.1080/17512549.2019.1612468; <https://www.tandfonline.com/doi/abs/10.1080/17512549.2019.1612468?journalCode=taer20&>.

Lu, X. and Memari, A. M., (2022). "Comparison of the Experimental Measurement Methods for Building Envelope Thermal Transmittance, MDPI Buildings, published 03/01/2022, Vol. 12, No. 3, 15p., <https://doi.org/10.3390/buildings12030282>.

Popescu, A., (2018). There's No Place Like Home, Especially If It's Made of Hemp. *The New York Times*, January 29, 2018, sec. Science. <https://www.nytimes.com/2018/01/29/science/hemp-homes-cannabis.html>.

Potter, B., (2020). "Every Building in America – an Analysis of the US Building Stock," *Construction Physics*, <https://constructionphysics.substack.com/p/every-building-in-america-an-analysis#:~:text=Using%20the%20sources%20above%2C%20we,containing%2040%20million%20housing%20units>.

Priesnitz, R., 2006. Hemp for Houses. *Natural Life Magazine*. <https://www.life.ca/naturallife/0604/hempouse.htm>.

Pullen, T., (2017). What Is Limecrete?. *Homebuilding & Remodeling*, March 8. <https://www.homebuilding.co.uk/what-is-limecrete/>.

Resistors, (2022). Available Online: [https://en.wikipedia.org/wiki/Resistor#:~:text=A resistor is a passive,transmission lines%2C among other uses;](https://en.wikipedia.org/wiki/Resistor#:~:text=A%20resistor%20is%20a%20passive,transmission%20lines%2C%20among%20other%20uses;) (Site visited 5/19/2022).

Silicone Heat Transfer Compound, (2022). Available Online: <https://www.walmart.com/ip/MG-Chemicals-860-60G-Silicone-Heat-Transfer-Compound-60g-Jar-Special-synthetic-base-fortified-metal-oxides-compounded-a-By-Brand/503050765?wmlspartner=wlpa&selectedSellerId=14995>; (Site visited 5/19/2022).

---

Telaire, (2022). Telaire CO2, Humidity, and Dust Sensors [https://www.amphenol-sensors.com/en/telaire?utm\\_term=&utm\\_campaign=dynamic&utm\\_source=google&utm\\_medium=ad&hsa\\_acc=5028947712&hsa\\_cam=6456478229&hsa\\_grp=77656162952&hsa\\_ad=491291535965&hsa\\_src=g&hsa\\_tgt=dsa-437115340933&hsa\\_kw=&hsa\\_mt=&hsa\\_net=adwords&hsa\\_](https://www.amphenol-sensors.com/en/telaire?utm_term=&utm_campaign=dynamic&utm_source=google&utm_medium=ad&hsa_acc=5028947712&hsa_cam=6456478229&hsa_grp=77656162952&hsa_ad=491291535965&hsa_src=g&hsa_tgt=dsa-437115340933&hsa_kw=&hsa_mt=&hsa_net=adwords&hsa_)

Texas Instruments, (2022). SBAS288K., (2003) – “Analog to Digital Converter (ADC),” <https://www.ti.com>, (Site visited 5/19/2022).

Thermistors, (2022). Available Online: <https://www.amazon.com/uxcell-Thermistors-Resistor-MF52-103-Temperature/dp/B07L113D>; (Site visited 5/19/2022).

Radical, (2019). “Building Lime Innovation,” [www.greenspec.co.uk/downloads/?filename=HemcreteR.pdf](http://www.greenspec.co.uk/downloads/?filename=HemcreteR.pdf); (Site visited May 2022).

# Appendix A. Blower Door (Air Leakage) Test

## PA Amended 2015 IECC Final Report



Harmony Home Energy  
 110 Oak Hill Drive  
 Harmony PA 16037  
 724-714-9220  
 michael@myharmonyhome.com

**DON Management**  
 Site location:  
 506 Spruce Street  
 New Castle PA 16101

Compliance path: *none selected*

### PA Amended 2015 IECC Infiltration Test

PA Amended IECC 2015 Required maximum 5 air changes per hour (ACH50)

Test Date: 05/04/2022  
 Test Result: **PASS**

Tested CFM50	Volume	Calculated ACH50
527	6416	4.93

Information entered reflect results at the time of testing. Any alterations to the home from the time of testing may alter results.  
 $ACH50 = (CFM50 \times 60 \text{ Minutes}) / \text{Volume}$

### PA Amended 2015 IECC Mechanical Ventilation Check

Test Date: 05/04/2022  
 Test Result: **Not Requested**

System Information:	System Location	Type	Rated CFM	Measured CFM
Conditioned Floor Area: 840 Number of Bedrooms: 1 Required Minimum Ventilation: 30	N/A	N/A	N/A	Not Measured

Fan Rated CFM used in determining code compliance. Bath Fan Efficacy 10-89 CFM (1.4CFM/watt) ,90CFM (2.8CFM/Watt). Verify at [www.hvi.org](http://www.hvi.org).  
 For AC Motor Fans use equation: Amps x volts x (.75 AC motor correction factor) = Watts if HVI certification is not available.

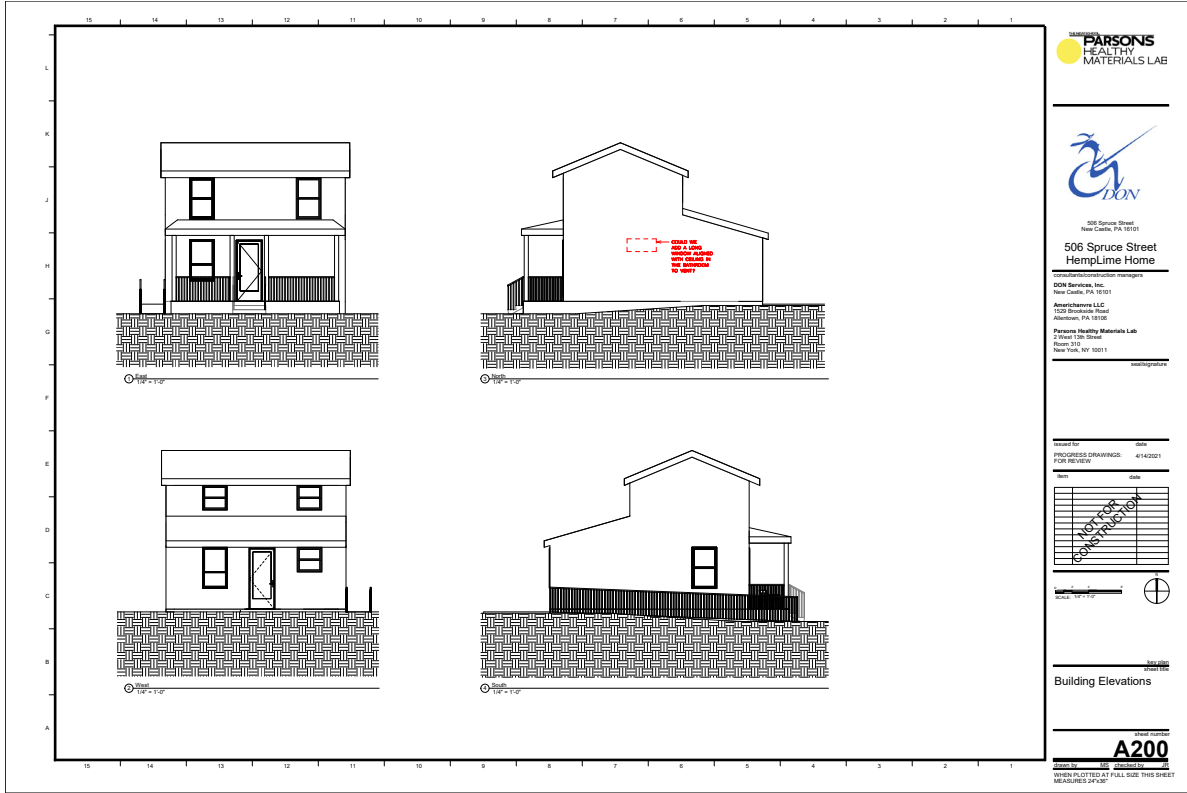
### PA Amended 2015 IECC Duct Leakage Test

Test Date: 05/04/2022  
 Test Result: **Not Requested**

	System #1	Duct Testing Requirements
Description	Not Requested	
Area Served	840.00	
Max Total Duct Leakage	NA	
Measured Total Leakage	NA	
Measured Total Leakage %	NA	
Measured Supply Leakage	NA	
Measured Return Leakage	NA	
Measured Leakage to Outside	NA	
Measured Leakage to Outside %	NA	
Max Total Duct Leakage %	NA	

Signature Michael J. Arblaster





PARSONS  
HEALTHY  
MATERIALS LAB



506 Spruce Street  
HempLime Home

Construction Manager  
DOM Services, Inc.  
New Castle, PA 16101  
Architects LLC  
1228 Brandywine Road  
Allentown, PA 18106  
Parsons Healthy Materials Lab  
Room 310  
New York, NY 10011

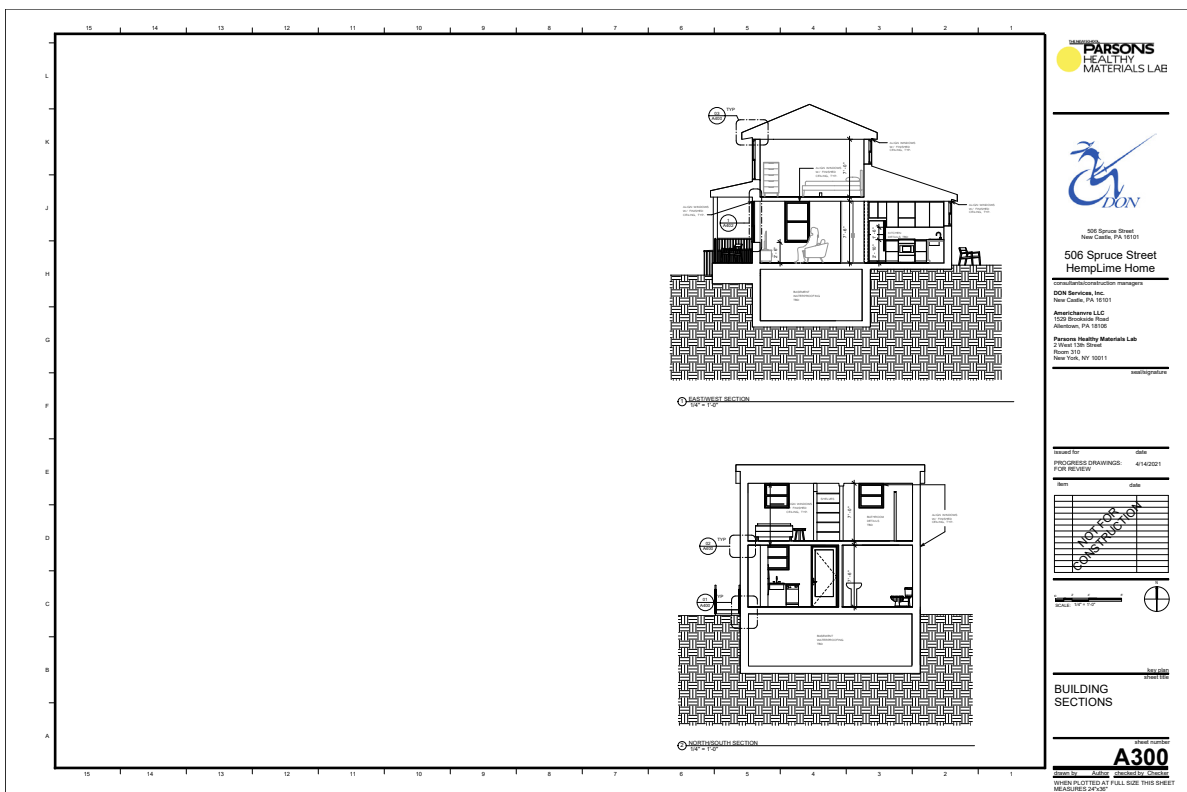
Issued for: date:  
PROCESS DRAWINGS: 4/14/2021  
FOR REVIEW

Rev	Date
<b>NOT FOR CONSTRUCTION</b>	



Building Elevations

Sheet number  
**A200**  
DATE: 4/14/2021  
BY: [signature]  
CHECKED BY: [signature]  
WHEN PLOTTED AT FULL SIZE THIS SHEET MEASURES 24"X36"



PARSONS  
HEALTHY  
MATERIALS LAB

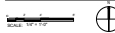


506 Spruce Street  
HempLime Home

Construction Manager  
DOM Services, Inc.  
New Castle, PA 16101  
Architects LLC  
1228 Brandywine Road  
Allentown, PA 18106  
Parsons Healthy Materials Lab  
Room 310  
New York, NY 10011

Issued for: date:  
PROCESS DRAWINGS: 4/14/2021  
FOR REVIEW

Rev	Date
<b>NOT FOR CONSTRUCTION</b>	



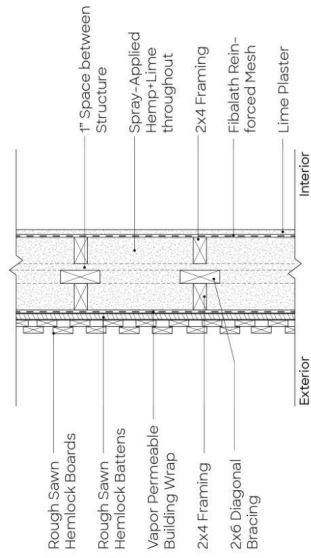
Building Sections

Sheet number  
**A300**  
DATE: 4/14/2021  
BY: [signature]  
CHECKED BY: [signature]  
WHEN PLOTTED AT FULL SIZE THIS SHEET MEASURES 24"X36"

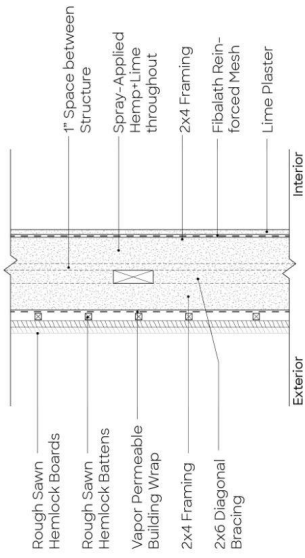




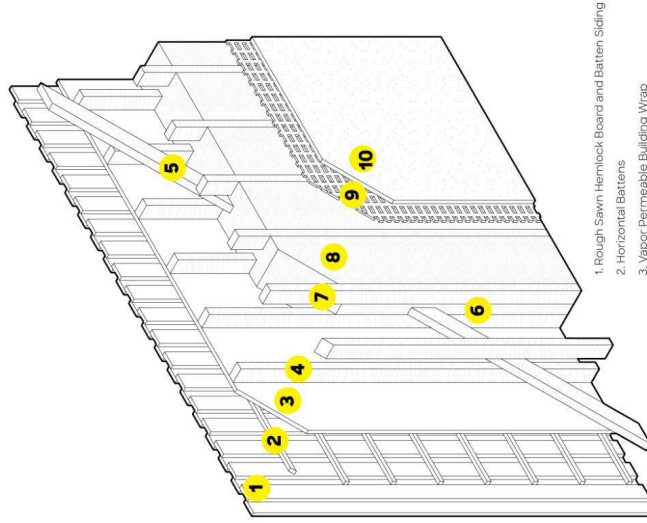
# Construction Details



**PLAN**



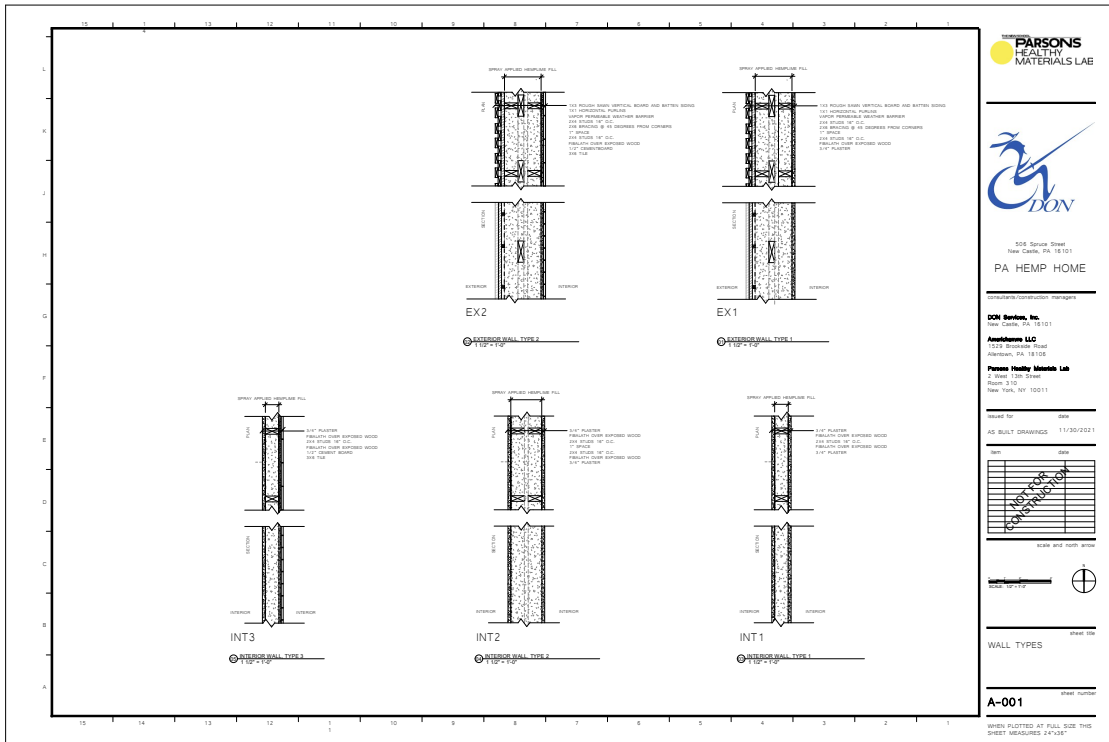
**SECTION**

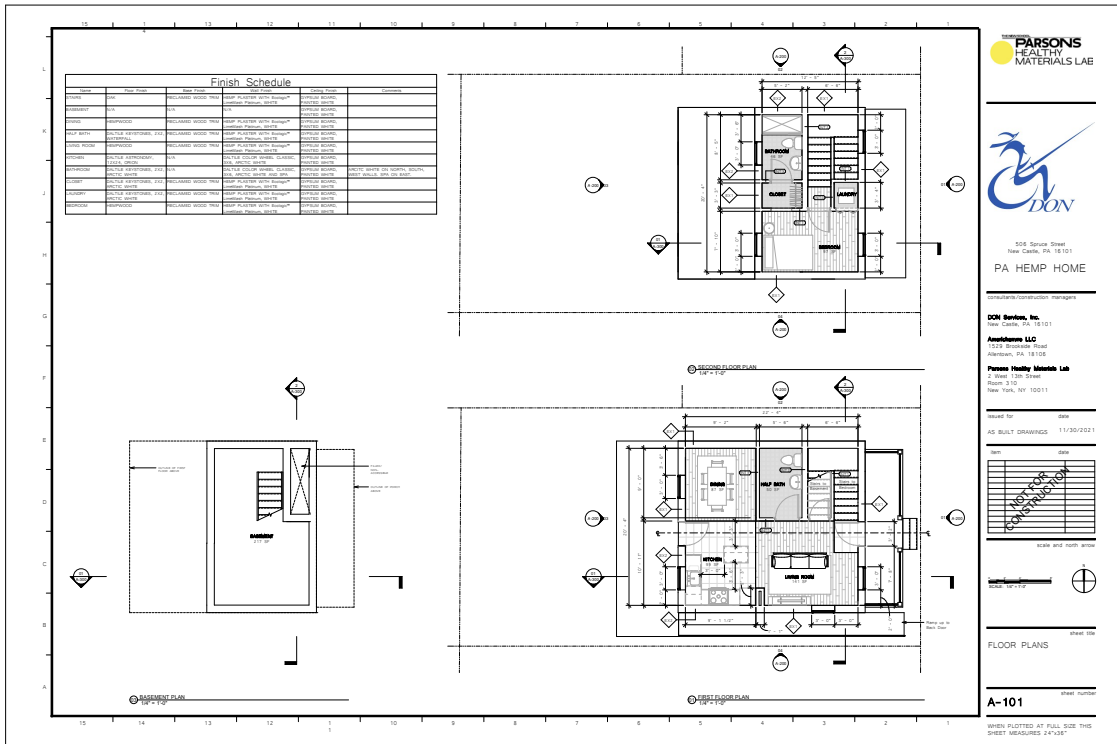
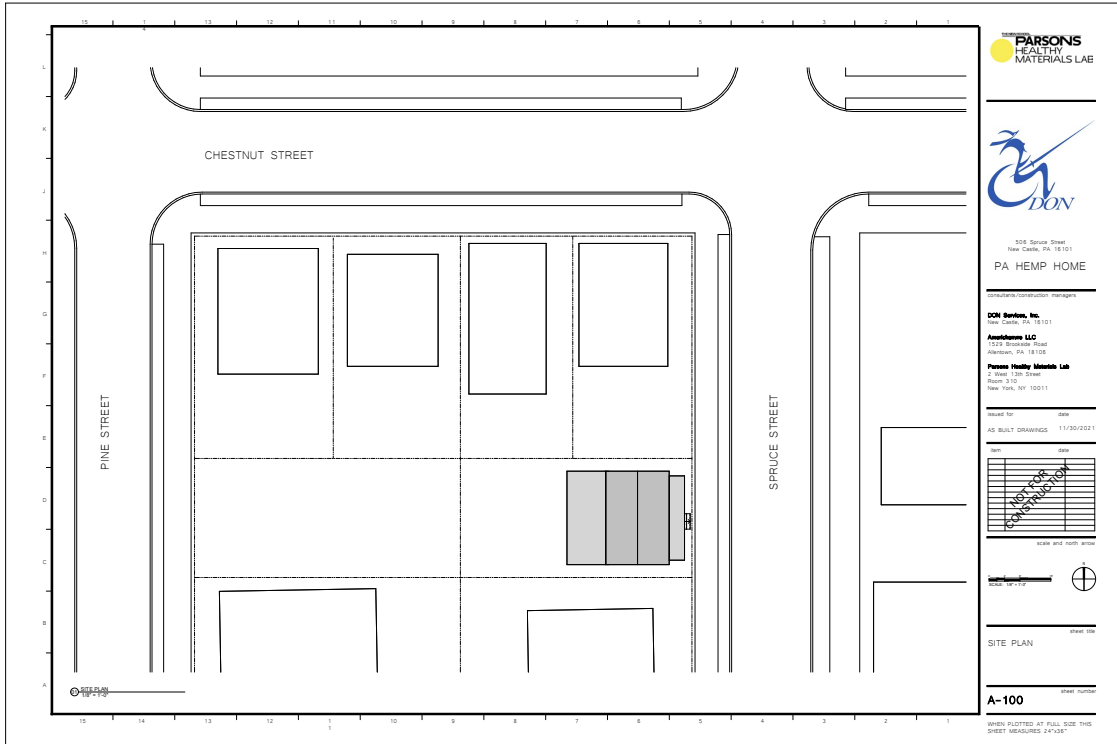


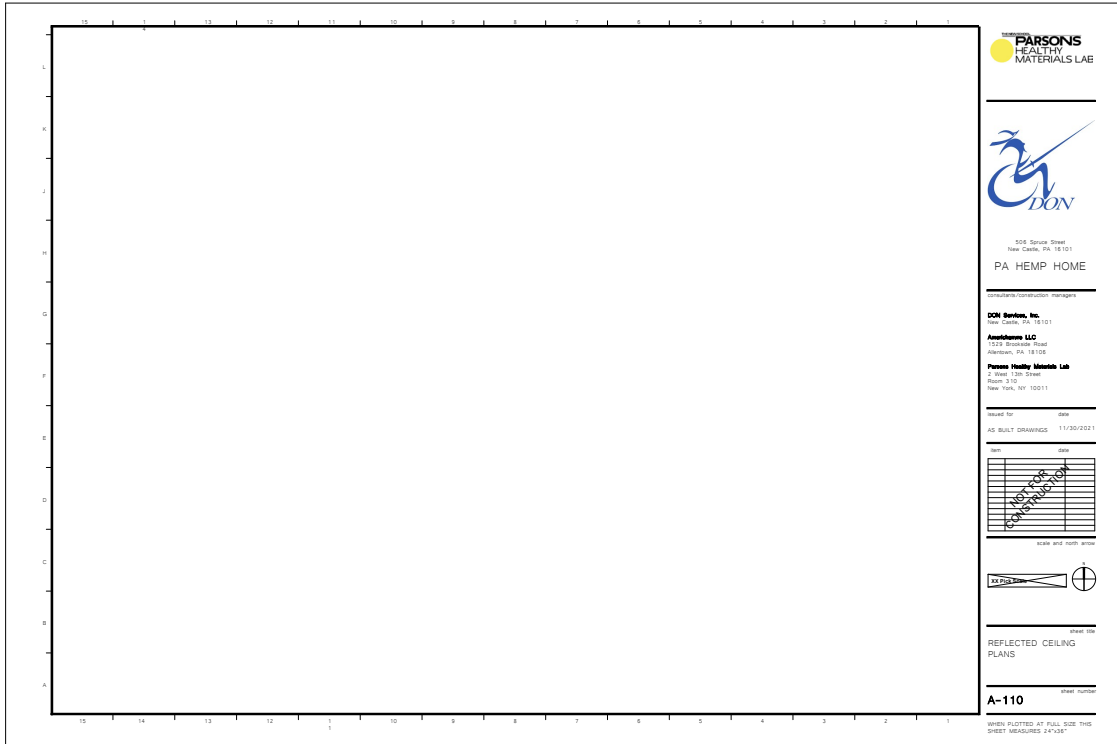
1. Rough Sawn Hemlock Board and Batten Siding
2. Horizontal Battens
3. Vapor Permeable Building Wrap
4. 2x4 Framing
5. 2x6 Diagonal Bracing
6. 1" Space between Structure
7. 2x4 Framing
8. Spray-Applied Hemp-Lime throughout
9. Fibalath Reinforced Mesh
10. Lime Plaster

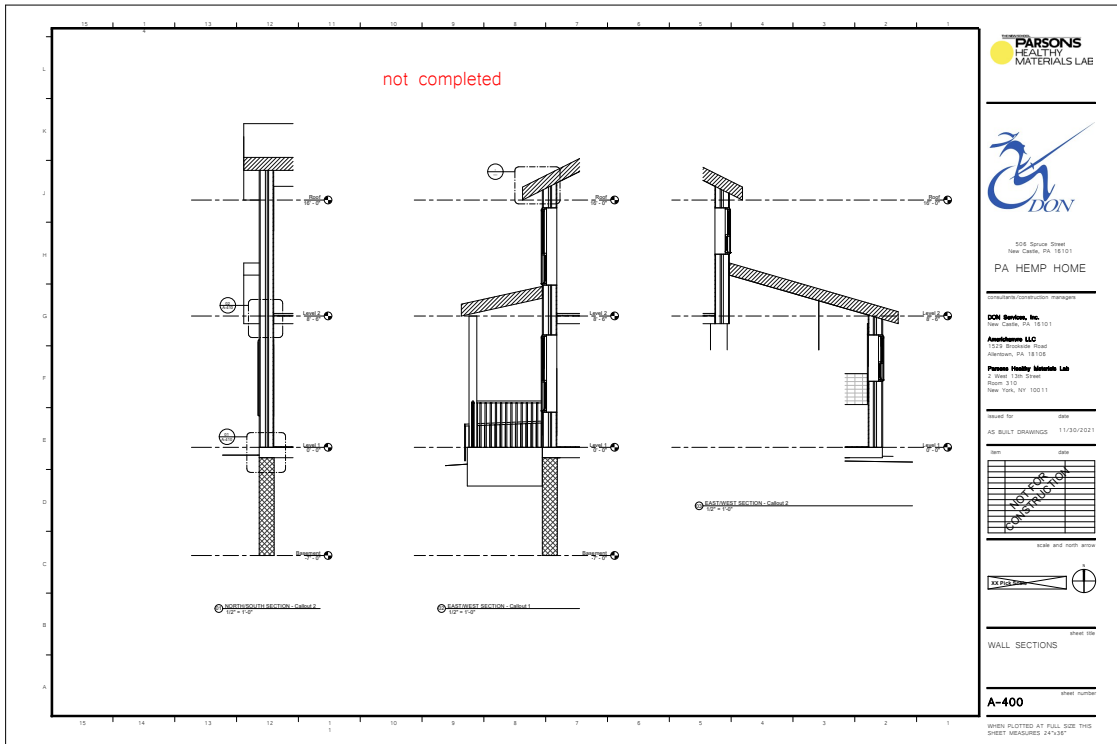
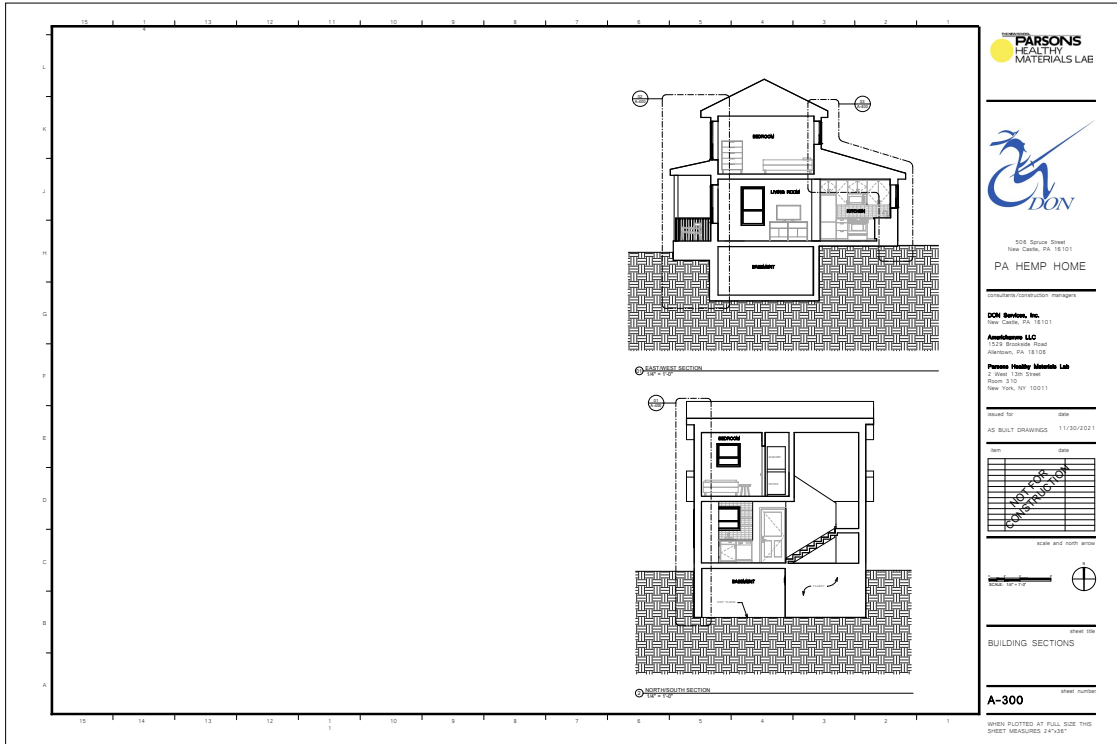


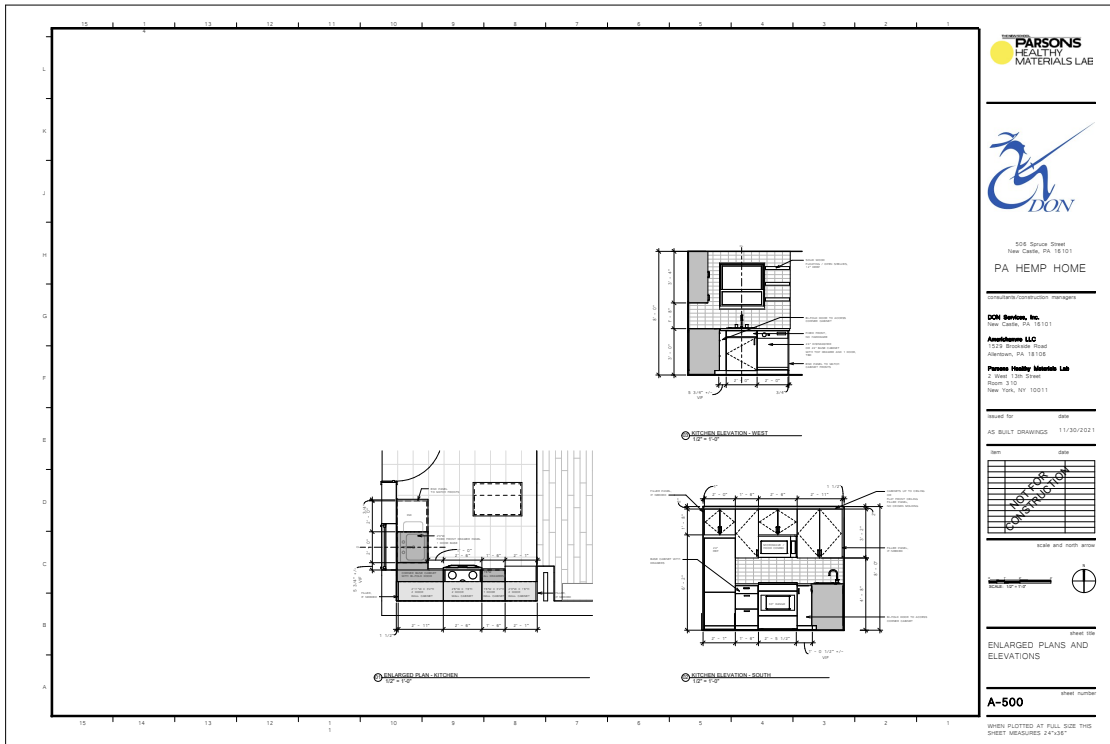
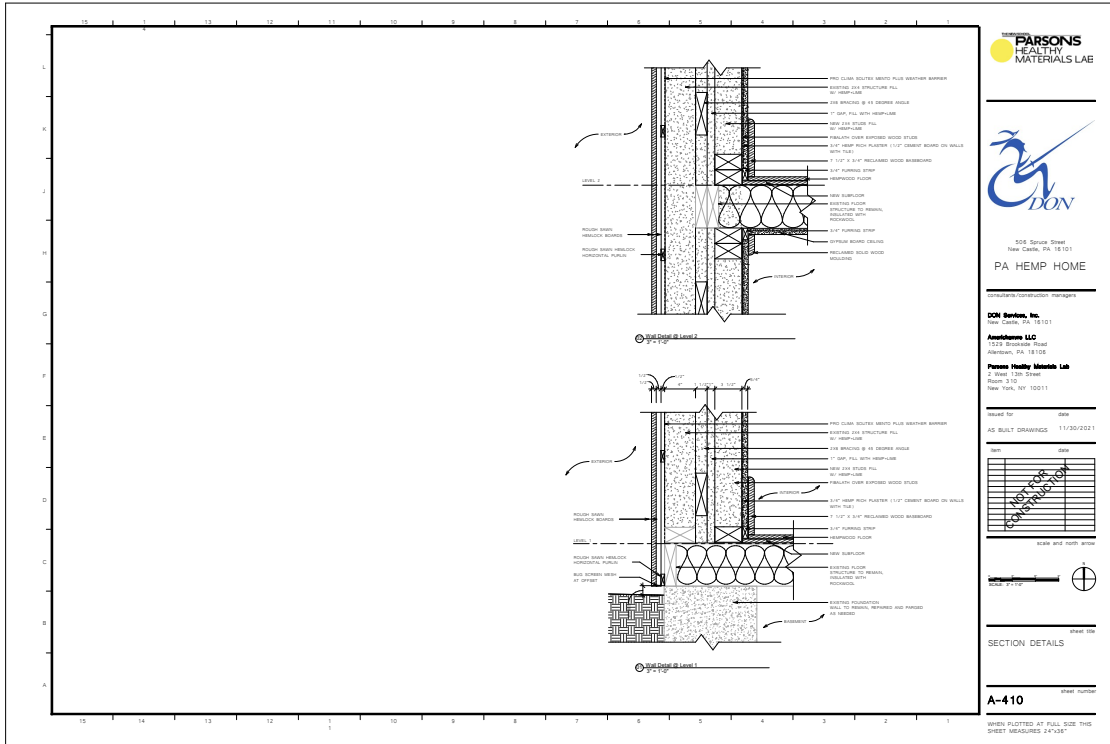
Sheet Name	Sheet Number
WALL TYPES	A-001
SITE PLAN	A-100
FLOOR PLANS	A-101
REFLECTED CEILING PLANS	A-110
BUILDING ELEVATIONS	A-200
BUILDING SECTIONS	A-300
WALL SECTIONS	A-400
SECTION DETAILS	A-410
ENLARGED PLANS AND ELEVATIONS	A-500











**Appendix C. Photos of Retrofitted House Prior to and during Finishing Interior / Exterior Surfaces**





























**PennState**  
College of Engineering

**PENNSYLVANIA HOUSING  
RESEARCH CENTER**